Characterization of organic aerosols from a Chinese Mega-City during winter: predominance of fossil fuel combustion

Md. Mozammel Haque[1,2,3], Kimitaka Kawamura[2], Dhananjay K. Deshmukh[2], Cao Fang[1, 3], Wenhuai Song[1,3], Bao Mengying[1,3] and Yan-Lin Zhang[1,3*]

[1] *Yale-NUIST Center on Atmospheric Environment, Department of Applied Meteorology, Nanjing University of Information Science and Technology, Nanjing 210044, China*
[2] *Chubu Institute for Advanced Studies, Chubu University, Kasugai 487-8501, Japan*
[3]*Key Laboratory of Meteorological Disaster, Ministry of Education & Collaborative Innovation Center on Forecast and Evaluation of Meteorological Disasters, Nanjing University of Information Science and Technology, Nanjing 210044, China*

Corresponding author
Yan-Lin Zhang
E-mail: dryanlinzhang@outlook.com

5 March, 2019

Abstract

$PM_{2.5}$ aerosol samples were collected from a Chinese mega-city in Nanjing (32.21°N and 118.73°E) during winter and analyzed for more than 100 compounds of twelve organic compound classes. The most abundant classes of compounds are *n*-alkanes (average, 205 ng m^{-3}), followed by fatty acids (76.3 ng m^{-3}), polycyclic aromatic hydrocarbons (PAHs) (64.3 ng m^{-3}), anhydro-sugars (56.3 ng m^{-3}), fatty alcohols (40.5 ng m^{-3}), and phthalate esters (15.2 ng m^{-3}), whereas hydroxy-/polyacids (8.33 ng m^{-3}), aromatic acids (7.35 ng m^{-3}), hopanes (4.19 ng m^{-3}), primary sugars and sugar alcohols (4.15 ng m^{-3}), lignin and resin products (2.94 ng m^{-3}), and steranes (2.46 ng m^{-3}) are less abundant. The carbon preference index of *n*-alkanes (0.83-1.38) indicated that they were significantly originated from the fossil fuels combustion. Diagnostic concentration ratios of organic tracers suggested that PAHs and hopanes are mostly originated from coal burning and traffic emissions, respectively in Nanjing urban area. Positive matrix factorization analysis demonstrated that fossil fuel combustion is the major source (28.7%) in Nanjing winter aerosols. Most of the compounds generally showed higher concentrations in nighttime compared to daytime, due to the accumulation process associated with the inversion layers and enhancement of emissions from heavy trucks at night. We conclude that fossil fuel combustion largely influences the winter organic aerosols in urban Nanjing area. Based on the comparison of present results with previous studies, we found that pollution levels on organic aerosols have been decreased in the urban Nanjing atmosphere for the last decade.

Keywords: $PM_{2.5}$, organic compounds, fossil fuel combustion, positive matrix factorization, Chinese urban aerosols.

1 Introduction

Particulate matter (PM) comprised a wide variety of chemical components, which are derived from a broad range of sources and processes in the atmosphere (Seinfeld and Pandis, 2006). Organic aerosol (OA) is one of the major constituents of airborne particulates, accounting for up to 70% of the fine aerosol mass. They can play a crucial role in the radiative forcing of the Earth and more generally to the environment (Kanakidou et al., 2005). In the last two decades, more attention has been paid to identify organic aerosol optical and cloud formation properties that link OA directly to hydrological cycle and thereby sustainability issues (Dusek et al., 2006; Riipinen et al., 2012). They can affect the climate, air quality, human health, visibility, and ecosystems on the local, regional and global scale (Salma et al., 2017). Several studies have reported that OA plays an important role in both the direct and indirect aerosol forcing, affecting the earth's radiation balance and global air quality (Cooke et al., 1999; Lohmann et al., 2000; Jacobson, 2001; Chung and Seinfeld, 2002). Aerosol particles improved with OM can make the aerosol surfaces more hydrophilic or hydrophobic based on the mixing state and aerosol composition, which further modify the CCN activities of particles. Furthermore, aerosols also influence air quality in addition to human health and climate, particularly in urban areas due to extensive anthropogenic emissions and favorable meteorological conditions (Watson, 2002).

There are two major sources of atmospheric aerosols that include both primary emissions and secondary aerosol formation. Primary organic aerosols (POA) are directly derived from various sources such as biomass burning, fossil fuels combustion, dust particles, microbial activities, and plant materials, etc., whereas secondary organic aerosols (SOA) are formed by the oxidation process of organic species in the atmosphere. Various types of volatile organic compounds (VOCs) are emitted from

natural and anthropogenic sources into the atmosphere. VOCs can be further photo-oxidized by OH, NO_x, O_3 to form SOA in the atmosphere (Haque et al., 2016). Both POA and SOA can contribute to the organic particulate matter (PM) formation in the atmosphere, which can significantly control the physicochemical properties of aerosol particles (Kanakidou et al., 2005). The chemical characterization and the contributions of various sources of aerosol particles are essential to figure out the role and potential impacts of OA in the atmosphere. Moreover, OA poses adverse physiological effects on human health causing asthma, bronchitis, cancer, and heart disease, etc. (Pope et al., 2009; Ramírez et al., 2011).

The large emissions of atmospheric particles from China have a major effect on regional and global climate changes (Huebert et al., 2003). Atmospheric pollution in China is a serious problem due to its rapid industrialization and urbanization. Globally, one-fourth of anthropogenic POA are originated in China (Cooke et al., 1999). Many studies have been performed to characterize inorganic aerosols from China due to the significant anthropogenic emissions. (Wang et al., 2011; He et al., 2012; Zheng et al., 2015; Li et al., 2017). However, studies on OAs of Chinese mega-cities are still poorly understood (Guo et al., 2003; Bi et al., 2003; Yao et al., 2003). Nanjing is a highly industrialized mega-city located in east China with a population of over 8 million where air pollution is a critical problem. Previous studies of Wang et al. (2002a; 2002b) reported that the aerosol mass of fine particles (< 2.5 μm) in Nanjing atmosphere was about 2-4 times higher than the United States Environmental Protection Agency (USEPA) regulations. The average concentrations of $PM_{2.5}$ were 66±33 μg m^{-3} in Nanjing aerosols during sampling period, whereas the Chinese Ambient Air Quality and WHO standard levels are 35 μg m^{-3} and 25 μg m^{-3}, respectively (Liu et al., 2016; Shen

et al., 2014), indicating that Nanjing air quality is still worse compared to China national and WHO standard levels.

The highest $PM_{2.5}$ concentrations were observed during winter in China due to the enhancement of anthropogenic emissions from fossil fuel combustion and biomass burning and unfavorable meteorological conditions, i.e., frequent development of inversion layers (Zhang et al., 2015). Ma et al. (2016) also reported $PM_{2.5}$ concentrations from 2004-2013 in China while winter was the most polluted season. To better understand the molecular composition and sources of OAs in Chinese urban area during winter, aerosol sampling campaign was carried on a day and night basis in the mega-city of Nanjing during winter period from 11 December 2014 to 11 January 2015. The objective of this study is to determine more than 100 organic compounds including aliphatic lipids, sugar compounds, polycyclic aromatic hydrocarbons (PAHs), hopanes, lignin and resin products, aromatic acids, polyacids, and steranes in the aerosol particles from Nanjing. Their chemical characteristics, diurnal patterns, and potential sources are discussed in comparison with previous studies conducted a decade ago.

2 Experimental

2.1 Sample collection

$PM_{2.5}$ sampling was performed from the rooftop of a six-story building at Nanjing University of Information Science and Technology, Nanjing, China using medium volume sampler (Laoshan, Quingdao, China) from 11 December 2014 to 11 January 2015 (Figure 1). Daytime and nighttime sampling was conducted from 9:30 to 21:00 and 21:30 to 9:00, respectively. Total of 62 samples was collected on prebaked (450°C for 6 h) quartz fiber filters (80 mm) with an air flow rate of 100 L min^{-1}. After sampling, the filter samples were wrapped with aluminum foil, transported to the laboratory and stored at -20°C until the analysis.

2.2 Analysis of polar organics

Several polar organic compounds containing COOH and OH groups were analyzed by gas chromatography-mass spectrometry (GC-MS) using solvent extraction followed by TMS-derivatization technique (Table S1). Filter aliquots (6.28 cm^2) were extracted three times with 5 mL of dichloromethane/methanol mixture (2:1) under ultra-sonication for 10 min. The solvent extracts were filtered through quartz wool packed in a Pasteur pipette to remove all insoluble matrixes, concentrated using a rotary evaporator under vacuum and then totally dried under a gentle nitrogen stream. The dried extracts were derivatized with 50 μL of N,O-bis-(trimethylsilyl)trifluoroacetamide (BSTFA) plus 1% trimethylsilyl chloride and 10 μL of pyridine in a glass vial (1.5 mL) with a Teflon-lined screw cap at 70°C for 3h. The C_{13} *n*-alkane (diluted in *n*-hexane) was used as an internal standard (1.43 ng μL^{-1}) prior to injection into a GC-MS for identification. Detailed information on the chemical analysis is interpreted elsewhere (Wang and Kawamura, 2005).

The derivatives were analyzed using Hewlett-Packard (HP) model 6890 GC coupled to an HP model 5973 mass-selective detector (MSD). The sample was injected into a splitless mode with the injector temperature at 280°C. The GC oven temperature was set at 50°C for 2 min and then increased from 50 to 120°C at 30°C min^{-1}, and then to 300°C at 6°C min^{-1} with a final isothermal hold at 300°C for 16 min. The GC separation was performed on a DB-5MS fused silica capillary column (30 m long × 0.25 mm inner diameter × 0.5 μm film thickness) with a carrier gas of helium (rate 1.0 mL min^{-1}). The mass spectrometer was conducted at 70 eV on an electron impact (EI) mode with a scan range from 50 to 650 Daltons (Da).

The organic components were determined by comparison with the retention times and mass spectra of authentic standards as well as literature and National Institute

of Standards and Technology (NIST) library data of mass fragmentation patterns (Medeiros and Simoneit, 2007). GC-MS relative response factor (RRF) of each compound was calculated using authentic standards and surrogate compounds. We performed a recovery experiment three times and acquired the average value of more than 80% for target compounds. The field blank filters (n = 5) were analyzed by the procedures as described above. The target species were not noticed in the blank filters. The analytical errors based on replicate analyses (n = 5) were <10%.

2.3 Analysis of nonpolar organics

Non-polar organics, including *n*-alkanes, PAHs, hopanes, and steranes were analyzed using thermal desorption gas chromatography-mass spectrometry (TD-GC-MS) technique. It should be noted that higher recoveries (>90%) were obtained for nonpolar organics using TD-GC-MS compared to TMS-derivatization/GC-MS (<70%) technique. The filter aliquots (3 mm diameter) were cut into two pieces and then placed into a TD quartz tube (78 mm long × 4 mm inner diameter) and spiked with internal standard mixture (isotope-labeled reference compounds) for quantification. The internal standards consisted of 3 deuterated PAHs, e.g., Nap-d_8, Ace-d_{10}, and Phe-d_{10}.

Thermal desorption was performed on an Agilent GC-MS system model 7890B/5977A. A capillary column (HP-5MS UI, 5% biphenyl/95% dimethylsiloxane, 30 m long × 0.25 mm inner diameter × 0.25 μm film thickness) was used to separate the target compounds. The GC oven temperature programmed from 35°C (3 min) to 120°C at 10°C min^{-1}, ramped from 120°C to 146°C at 4°C min^{-1} and continued to 310°C at 8°C min^{-1}, then held at 310°C for 16 min. The sample on the filter punch was inserted into the TD tube with the initial temperature at 35°C before running and increased up to 300°C manually at 12°C sec^{-1} after starting the analysis. Column flow rate was 2 mL min^{-1} and split flow was 10 mL min^{-1} for the first 3 mins, then column and split flow

rate changed to 1 mL min^{-1} and 25 mL min^{-1}, respectively. The electron ionization mass spectra (70 eV) were conducted on a scan mode range from 50 to 650 Da. The temperatures of the ion source, quadruples and transfer line were set at 310, 150 and 310°C, respectively.

2.4 Carbonaceous components analysis

Organic carbon (OC) and elemental carbon (EC) were measured using a Sunset Laboratory carbon analyzer following the IMPROVE (Interagency Monitoring of Protected Visual Environments) thermal-optical evolution protocol and assuming carbonate carbon to be insignificant in the sample (Boreddy et al., 2018). An area of 1.54 cm^2 of each quartz filter sample was insert in a quartz boat inside the thermal desorption chamber of the analyzer, and then stepwise heating was performed.

A filter cut of 3.14 $cm^2$of each sample was extracted with 20 mL organic-free ultrapure water (resistivity >18.2 MΩ cm, Sartorius arium 611 UV) under ultrasonication for 30 min. The water extracts were then passed through a membrane disc filter to throw away the insoluble filter matrixes and analyzed for water-soluble organic carbon (WSOC) using a total organic carbon (TOC) analyzer (Shimadzu, TOC-Vcsh) (Boreddy et al., 2018). The analytical errors in the triplicate analyses were within 5% for all carbonaceous components and the concentrations reported here were corrected for the field blanks.

2.5 Major inorganic ion analysis

An area of 5.07 cm^2 of each quartz filter sample was extracted with 10.0 mL ultrapure water (> 18.2 Ω) under ultrasonication (30 min). The extract solution was filtered through a membrane disc filter (Millex-GV, Millipore) of pore size 0.22 μm to remove insoluble materials, then analyzed for inorganic ions using ion chromatography on a Thermo Fisher Scientific ICS-5000 (America) equipped with a gradient pump

(SP), a conductivity detector/chromatography compartment (DC) and an automated sampler (AS-DV). The cations were measured by an Ion Pac CS12A analytical column and an Ion Pac CG12A guard column with an eluent of aqueous methanesulfonic acid (MSA, 30 mM L^{-1}) and a flow rate of 1 mL min^{-1}. In contrast, anions were separated on an Ion Pac AS11-HC analytical column and an Ion Pac AG11-HC guard column with an eluent of sodium hydroxide (NaOH) gradient at a flow rate of 1.5 mL min^{-1} (0-3 min, 0.5 mM L^{-1}; 3-5 min, 0.5-5 mM L^{-1}; 5-15 min, 5-30 mM L^{-1};15-20 min 0.5 mM L^{-1}).

3 Results and Discussion

3.1 Diurnal variations and meteorological conditions

No significant difference was observed between day- and night-time for organic compounds in winter aerosols from Nanjing urban area (Figure 2, Tables 1 and S1). Nevertheless, concentrations of organic compounds in nighttime were slightly higher than daytime in most of the cases. It is notable that the planetary boundary layer height (PBLH) is generally lower in nighttime than daytime causing higher concentrations of aerosol particles at night. Interestingly, we found high loadings of organics in daytime sample collected on 15 December when PBLH was high (632 m), whereas lower levels of organics were observed in nighttime of 14 December (PBLH = 82.2 m) (Figures 3 and S1b).

We observed one episode (E1) during 2 - 5 January while $PM_{2.5}$ and all organic compounds showed similar temporal variations with high loadings (Figure 3). Fascinatingly, NO_2 showed high concentration during E1, whereas relative humidity (RH) and ozone (O_3) levels were not high (Figure S1). Our results suggest that NO_2 influences the organic molecular compositions in urban aerosols. It is noteworthy that the major source of NO_2 is of vehicular exhaust origin (Kendrick et al., 2015). However, coal combustion can also emit NOx into the atmosphere (Chang et al., 2018).

Previous studies also reported that NO_x could affect SOA formation (Kanakidou et al., 2005; Zhang et al., 2015; Mochizuki et al., 2015). Moreover, PAHs, hopanes, and steranes showed another episode on 23 and 24 December 2014 probably due to the coal combustion event. It should be noted that higher RH (81-88%) and $PM_{2.5}$ levels (152-226 μg m^{-3}) cause less visibility on 29 December (1.7 km), 10 January (1.8 km), and 11 January (1.6 km), which might be due to the haze formation. It is remarkable that the levels of organics were not high during these periods (Figures 3 and S1). These results imply that NO_2 derived from fossil fuel combustion plays an important role in the formation of OAs in the Nanjing atmosphere.

3.2 Carbonaceous components

The results of OC, EC, and WSOC are mentioned in Table 1. The values of OC and EC were found to be 8.76-40.0 μg m^{-3} (ave. 18.6 μg m^{-3}) and 2.41-30.3 μg m^{-3} (8.25 μg m^{-3}) in daytime, and 2.98-40.1 μg m^{-3} (19.1 μg m^{-3}) and 0.87-22.9 μg m^{-3} (8.86 μg m^{-3}) in nighttime, respectively. We found that the day and night variations of OC and EC values are also not significant. The mass ratio of OC to EC (OC/EC) is often used to characterize fossil fuels and biomass burning emissions. Several investigators have used OC/EC ratios to classify the sources of carbonaceous aerosols (Ram et al., 2008; Sandradewi et al., 2008; Saarikoski et al., 2008). The higher OC/EC ratios imply that major source of carbonaceous species is from biomass burning, whereas lower ratios are characteristics of emissions from fossil fuels combustion. Sandradewi et al. (2008) have documented an average OC/EC ratio of 1.1 for vehicular emission and 7.3 for wood burning emission. Saarikoski et al. (2008) pointed out OC/EC ratios of 0.71 for vehicular emission and 6.6 for biomass burning. Watson et al. (2001) proposed the OC/EC ratios of 1.1 for vehicular emission, 2.7 for coal combustion and 9.0 for biomass burning emission. The OC/EC ratios ranged from 1.30 to 3.80 with a mean value of

253 2.40 in this study, which is comparable to the values reported for coal combustion and
254 vehicular emission. These results suggest that fossil fuel combustion is the major source
255 of carbonaceous aerosols in urban Nanjing.

256 The ratios of OC to EC are also used to differentiate the relative contribution of
257 primary vs. secondary sources; high OC/EC ratios (>2.0) were reported for the aerosols
258 with significant contributions of SOA (Kunwar and Kawamura, 2014; Pani et al., 2017).
259 The OC/EC ratio in this study was on average 2.40, suggesting the significant
260 contribution of SOA in Nanjing aerosols that is consistent with PMF results (see section
261 3.4). The concentration range of WSOC was 5.52-26.6 μg m^{-3} (11.7 μg m^{-3}) in daytime
262 and 2.51-20.2 μg m^{-3} (11.8 μg m^{-3}) in nighttime. The WSOC/OC ratios often used to
263 discuss the SOA formation via photochemical aging of atmospheric aerosol particles.
264 The WSOC/OC ratios exceeding 0.4 indicate the aged aerosols with the significant
265 contribution of SOA (Boreddy et al., 2018). The average WSOC/OC ratio of 0.64 in the
266 present study indicates that OAs in Nanjing were relatively aged**.** Moreover, air mass
267 back trajectories also indicate that some air masses come from the polluted regions over
268 North China, suggesting a SOA formation during long-range transport (Figure S5).

269 **3.3 Organic molecular compositions**

270 We detected twelve organic compound classes, including sugars, lignin and
271 resin acids, fatty acids, fatty alcohols, *n*-alkanes, PAHs, hopanes, steranes, glycerol and
272 polyacids, phthalate esters, and aromatic acids in the aerosol samples from Nanjing. The
273 total concentrations of organics were on average 424 ng m^{-3} in daytime and 555 ng m^{-3}
274 in nighttime with the predominance of *n*-alkanes followed by fatty acids, PAHs,
275 anhydro-sugars, fatty alcohols, phthalate esters, glycerol and polyacids, aromatic acids,
276 sugars, hopanes, lignin and resin acids, and steranes (Figure 2). Table S1 shows the

277 values of identified organic compounds. Levoglucosan was the single dominant species
278 followed by C_{16} and C_{24} fatty acids, and C_{29} *n*-alkane (Table S1).

279 **3.3.1 Aliphatic lipid components**

280 The lipid compounds, e.g., fatty acids, fatty alcohols, and *n*-alkanes are mainly
281 originated from marine or microbial detritus, terrestrial higher plant waxes, and fossil
282 fuels combustion. Homologues of *n*-alkanes (C_{13}-C_{39}) were detected with higher
283 concentrations in nighttime (74.8-535 ng m^{-3}, ave. 228 ng m^{-3}) than daytime (97.6-497
284 ng m^{-3}, 184 ng m^{-3}) with a maximum at C_{29} (14.0 ng m^{-3} during daytime and 17.9 ng m^{-3}
285 during nighttime) in Nanjing aerosols (Tables 1 and S1, Figure 4a). These
286 concentrations are comparable to those reported from urban cities in Hong Kong (195
287 ng m^{-3}) and Shanghai (259 ng m^{-3}) (Wang et al., 2006), but much higher than the
288 western North Pacific region (0.11-14.1 ng m^{-3}) (Kawamura et al., 2003). Concentration
289 levels of *n*-alkanes in this study are not significantly different from previous studies in
290 Nanjing (112-265 ng m^{-3}, 172 ng m^{-3} during daytime; 61.0-503 ng m^{-3}, 278 ng m^{-3}
291 during nighttime) (Table 2) (Wang and Kawamura, 2005).

292 Biogenic *n*-alkanes showed stronger odd/even carbon number predominance
293 with a carbon preference index (CPI) of >5, whereas anthropogenic *n*-alkanes CPI value
294 is usually close to unity (Simoneit et al., 1991a, 2004c). CPI values obtained in this
295 study ranged from 1.18-1.32 (ave. 1.28) in daytime and 1.10-1.37 (1.24) in nighttime,
296 which is close to unity. This result suggests that the major contributor of *n*-alkanes is
297 the anthropogenic activity such as fossil fuels combustion with less contribution from
298 higher plants in Nanjing aerosols. The present CPI values are similar with those from
299 other Chinese urban areas (ave. 1.16) (Wang et al., 2006) and Tokyo (1.10-2.80, ave.
300 1.50) (Kawamura et al., 1995). On the contrary, higher CPI values were reported for
301 Mt. Tai (4.60) (Fu et al., 2008) and Chichi-jima aerosols (4.50) (Kawamura et al.,

2003), where *n*-alkanes were mainly originated from terrestrial higher plant waxes. Plant wax derived *n*-alkanes are estimated as the excess of odd homologues minus adjacent even homologues (Simoneit et al., 1991b, 2004c), which is attributable to vascular plant waxes (Tables 1 and S1). Concentrations ranges of higher plant wax derived *n*-alkanes were 2.12-48.1 ng m^{-3} (ave. 15.5 ng m^{-3}) in daytime and 0.86-58.9 ng m^{-3} (17.6 ng m^{-3}) in nighttime, both of which are much lower than total *n*-alkanes, indicating that *n*-alkanes in Nanjing urban area are derived mainly from fossil fuel combustion.

A homologous series of $C_{12:0}$-$C_{32:0}$ saturated fatty acids, including two unsaturated fatty acids ($C_{18:1}$ and $C_{18:2}$), were identified in Nanjing samples. The values of total fatty acids ranged from 14.3 to 254 ng m^{-3} (ave. 66.8 ng m^{-3}) during daytime, whereas they ranged from 8.59 to 252 ng m^{-3} (91.3 ng m^{-3}) during nighttime. It is notable that fatty acids are less abundant compared to *n*-alkanes in Nanjing samples (Figure 2). The molecular distributions of fatty acids are observed by a strong even carbon number predominance with C_{max} at $C_{16:0}$ and $C_{24:0}$ (Table S1 and Figure 4b). CPI values of fatty acids are found to be 5.41 in daytime and 5.52 in nighttime samples. A similar distribution pattern has been proposed in marine and continental aerosols (Mochida et al., 2002; Kawamura et al., 2003; Fu et al., 2008). LMW fatty acids ($<C_{20:0}$) are originated from various sources, e.g., vascular plants, microbial sources, and marine phytoplankton, while HMW fatty acids ($>C_{20:0}$) are derived from terrestrial higher plant waxes (Kawamura et al., 2003; Kolattukudy, 1976; Simoneit, 1978). Biomass burning, motor vehicles, and cooking can also be the important sources of fatty acids in urban areas (Fu et al., 2010). The values of $C_{18:1}$ was observed lower in daytime than nighttime, suggesting an enhanced emission to the atmosphere and oxidation with a higher rate in daytime (Kawamura and Gagosian, 1987).

Concentration ranges of C_{12}-C_{34} fatty alcohols were 7.30-165 ng m^{-3} (ave. 36.9 ng m^{-3}) during daytime and 4.61-129 ng m^{-3} (43.8 ng m^{-3}) during nighttime (Table S1 and Figure 2). Their molecular distributions are characterized by a strong even-to-odd carbon number predominance with C_{max} at C_{28} or C_{30} (Figure 4c). We found that the CPI values of fatty alcohols in Nanjing aerosols (2.56-10.3, ave. 5.22 in daytime and 3.06-15.5, 6.32 in nighttime) are lower than those of aerosols from Chennai, India (9.75±2.94) (Fu et al., 2010) and Mt. Tai, China (CPIs 7.95-66.5, ave. 25.6 in daytime and 12.2-53.4, 22.8 in nighttime) (Fu et al., 2008). HMW fatty alcohols (>C_{20}) are dominant in the terrestrial higher plant, soils, and loess deposits, whereas LMW fatty alcohols (<C_{20}) are dominant in marine biota and soil microbes (Simoneit et al., 1991b). Moreover, a large amount of fatty alcohols together with fatty acids and *n*-alkanes can also be derived from biomass burning (Simoneit, 2002). A positive correlation was observed between fatty alcohols and levoglucosan ($r = 0.60$, $p<0.001$), indicating that fatty alcohols are partly originated from biomass burning in Nanjing winter aerosols (Figure S2c). This conclusion is further supported by the factors resolved by PMF analysis, where high loading of fatty alcohols was found with a biomass burning tracer levoglucosan.

3.3.2 Biomass burning tracers

Levoglucosan, galactosan, and mannosan are class of anhydro-sugars, which are produced by the pyrolysis of cellulose and hemi-cellulose (Simoneit, 2002). Levoglucosan is a unique tracer of biomass burning, and has been reported in urban (Wang et al., 2006; Fu et al., 2010; Yttri et al., 2007), marine (Simoneit et al., 2004b; Ding et al., 2013), and polar regions (Stohl et al., 2007; Fu et al., 2009). Levoglucosan is a relatively stable species in the atmospheric aerosol and could be transported long distances (Mochida et al., 2010). We found that levoglucosan is one of the most

352 abundant single tracer among all the identified compounds in the presents study, with a
353 concentration range of 4.79-179 ng m^{-3} (ave. 38.4 ng m^{-3}) during daytime and 4.96-354
354 ng m^{-3} (66.0 ng m^{-3}) during nighttime (Tables 1 and S1, Figure 5a), although the values
355 are lower than previous results reported in Nanjing (Wang and Kawamura, 2005).

356 Levoglucosan could account for up to 90% of total sugars in Chinese urban
357 aerosols (Wang et al., 2006). The contribution of levoglucosan to OC and WSOC were
358 0.02-0.51% (ave. 0.09%) and 0.03-0.57% (0.13%) in daytime and 0.02-0.48% (0.13%)
359 and 0.03-0.78% (0.22%) in nighttime, respectively. Galactosan and mannosan were also
360 detected in the aerosol samples. The amounts of galactosan were found to be 0.65-7.47
361 ng m^{-3} (ave. 2.26 ng m^{-3}) in daytime and 0.48–7.75 ng m^{-3} (3.13 ng m^{-3}) in nighttime,
362 whereas those of mannosan were 0.36-4.30 ng m^{-3} (1.62 ng m^{-3}) in daytime and 0.27-
363 5.73 ng m^{-3} (2.06 ng m^{-3}) in nighttime (Table S1 and Figure 5a). Levoglucosan showed
364 similar temporal trends and strong correlations with galactosan ($r = 0.87$, $p<0.001$) and
365 mannosan ($r = 0.84$, $p<0.001$) (Figure S2a). It should be noted that the levoglucosan
366 level in this study is 4-6 times lower than that of a previous study in Nanjing (Table 2)
367 (Wang and Kawamura, 2005). This result implies that biomass-burning emissions have
368 been decreased significantly in the last decade in the Nanjing area during winter.

369 We detected four lignin and resin products, i.e., 4-hydroxybenzoic, vanillic,
370 syringic, and dehydroabietic acids, which have been used as biomass-burning tracers
371 (Simoneit et al., 2004c). Lignin is a wood polymer, which can produce phenolic acids
372 during burning whereas dehydroabietic acid is more specific to conifer resin (Simoneit,
373 2002). We found that 4-hydroxybenzoic acid was dominant among all lignin and resin
374 products identified in Nanjing samples (Figure 5b). The concentration ranges of 4-
375 hydroxybenzoic, vanillic and syringic acids in day- and night-time were 0.65-4.31 ng m^{-3}
376 (ave. 1.80 ng m^{-3}) and 0.62-4.96 ng m^{-3} (2.01 ng m^{-3}), 0.04-0.92 ng m^{-3} (0.25 ng m^{-3})

and 0.08-0.66 ng m^{-3} (0.25 ng m^{-3}), and 0.04-0.57 ng m^{-3}(0.17 ng m^{-3}) and 0.05-0.43 ng m^{-3} (0.20 ng m^{-3}), respectively. The value of dehydroabietic acid was observed 0.11-1.16 ng m^{-3} (0.46 ng m^{-3}) during daytime and 0.00-8.29 ng m^{-3} (0.93 ng m^{-3}) during nighttime. The levels of lignin and resin acids in this study are 1-10 orders of magnitude lower than those from India (Fu et al., 2010) and China (Wang et al., 2006). Lignin products showed strong correlations with levoglucosan ($r = 0.60$-0.72, $p<0.001$), suggesting the similar sources and origins. In contrast, there is no correlation of dehydroabietic acid with levoglucosan ($r = 0.07$), indicating a different source of dehydroabietic acid in Nanjing aerosols. The low concentrations of dehydroabietic acid imply that boreal conifer forest fires are not important for the Nanjing aerosols.

3.3.3 Primary sugars and sugar alcohols

Sugar compounds are considered as tracers for primary biological aerosol particles, which are water-soluble and thus contribute to WSOC in aerosol particles (Elbert et al., 2007; Medeiros et al., 2006; Yttri et al., 2007). Four primary sugars (glucose, fructose, trehalose, and sucrose) and four sugar alcohols (erythritol, arabitol, mannitol, and inositol) were identified in the aerosol samples from Nanjing. The sugar compounds are generated from micro-organism (pollen, fungi, and bacteria), plants, flowers, resuspension of surface soil and unpaved road dust (Graham et al., 2003; Simoneit et al., 2004a; Yttri et al., 2007). They can also be originated during biomass burning. Total concentrations of primary sugars measured were 0.78-7.02 ng m^{-3} (ave. 2.90 ng m^{-3}) in daytime and 0.50-6.58 ng m^{-3} (2.98 ng m^{-3}) in nighttime, whereas those of sugar alcohols were 0.30-2.90 ng m^{-3} (1.16 ng m^{-3}) during daytime and 0.19-2.75 ng m^{-3} (1.27 ng m^{-3}) during nighttime.

Most primary sugars exhibited higher concentrations in daytime than nighttime except for glucose (Figure 5c). Graham et al. (2003) proposed that fructose and glucose

along with sucrose are emitted as fern spores, pollen, and other "giant" bioaerosol particles in daytime. Glucose showed a significant correlation with levoglucosan ($r = 0.75$, $p<0.001$) (Figure S2d), indicating that it is associated with biomass burning, which can interpret high levels of glucose in nighttime, whereas other primary sugars showed weak correlations with levoglucosan ($r = 0.05$-0.09). Biomass burning as a source of glucose has also been proposed by Fu et al. (2008). Trehalose is mostly derived from microorganisms such as bacteria, fungi, and yeast and also small amount from higher plants, and invertebrates (Medeiros et al., 2006). It is also considered as a product of unpaved road dust and resuspension of surface soil (Simoneit et al., 2004b; Wang and Kawamura, 2005).

On the contrary, all sugar alcohols presented higher concentrations in nighttime than in daytime while the scenario is opposite for primary sugars. Significant correlations were observed between sugar alcohols and levoglucosan ($r = 0.51$-0.75, $p<0.001$), suggesting a contribution of biomass burning to primary bio-aerosol particles, which can explain their higher concentrations in nighttime. Previous articles proposed that a huge amount of sugars and sugar alcohols can be emitted through the combustion of green vegetation from temperate forests (Medeiros and Simoneit, 2008). The sugar polyols are produced mainly from microbial sources, e.g., fungi, bacteria. They can also release from the bark of trees, leaves, and branches. The values of sugar compounds in this study are lower than other Chinese urban areas (Wang et al., 2006).

3.3.4 Polycyclic aromatic hydrocarbons

PAHs have severe health effect due to their genotoxicity and carcinogenicity. These aromatic compounds are mainly emitted from anthropogenic activities, including biomass burning, coal combustion, vehicular emissions, and natural gas combustion. PAHs showed a weak positive correlation with levoglucosan ($r = 0.20$), suggesting that

there is no serious contribution of PAHs from biomass burning activities in Nanjing aerosols. Total seventeen PAHs were identified in the Nanjing samples with the concentration range of 29.5-106 ng m^{-3} (ave. 54.5 ng m^{-3}) in daytime and 21.7-223 ng m^{-3} (72.5 ng m^{-3}) in nighttime (Tables 1 and S1, Figure 2). The higher concentrations of PAHs in nighttime might be due to the lower dispersion of the boundary layer at night (Figure 6a). Furthermore, households coal combustion has a significant contribution to the air quality in China during winter (Kerimray et al., 2017). Temperature falls down during nighttime resulting in the uses of a large amount of coal for house heating in a rural area due to a cold weather. Heavy-duty trucks that are permitted by the local government to work only at night as well as coal combustion should contribute to higher concentrations of PAHs into the air in nighttime. Our values are 3-4 times higher than those found in Hong Kong (14 ng m^{-3}) but lower than those in Beijing winter aerosols (208 ng m^{-3}) (Wang et al., 2006). Fluoranthene was found as a dominant PAH (ave. 8.24 ng m^{-3}) in Nanjing aerosol samples followed by chrysene (6.72 ng m^{-3}), pyrene (6.42 ng m^{-3}) and benzo(b)fluoranthene (BbF) (5.85 ng m^{-3}) (Figure 6a).

PAHs can be further photooxidized to form SOA, i.e., phthalic acid in the atmosphere (Zhang et al., 2016). Ding et al. (2007) proposed that PAHs could be degraded during long-range transport. Therefore, the ratios of PAH isomer pairs can be used to interpret the chemical aging of PAHs in the atmosphere. Benzo[a]anthracene (BaA) and benzo(a)pyrene (BaP) are expected to be degraded more easily than their isomers during transportation due to their higher reactivity. Thus, the lower ratios (<1.0) of benzo[a]anthracene (BaA)/chrysene (Chry) and benzo(a)pyrene (BaP)/ benzo(e)pyrene (BeP) indicate relatively more photochemical processing of PAHs. The ratios of BaA/Chry and BaP/BeP were calculated 0.79 and 0.88, respectively, which

imply that PAHs of Nanjing aerosols were more aged due to the atmospheric transportation from long distances.

Characteristic ratios of PAHs are indicative of their specific sources. Previous studies (Wang et al., 2007a, 2009; Bi et al., 2005) pointed out that the concentration ratios of indeno(1,2,3-cd)pyrene to benzo(ghi)perylene (IP/BghiP), and benzo(ghi)perylene to benz(e)pyrene (BghiP/BeP), are indicative of different emission sources (Table 3). The ratios of IP/BghiP nearby 0.22, 0.50 and 1.3 are attributable to gasoline, diesel, and coal combustion sources, respectively. On the other hand, BghiP/BeP ratio of 2.0 indicates mobile exhausts and 0.8 indicates coal combustion emissions (Grimmer et al., 1983; Ohura et al., 2004). Furthermore, the fluoranthene/(fluoranthene+pyrene) (Flut/(Flut + Pyr)) ratios of 0.46-0.56 indicate vehicular emissions, especially from catalytic converter-equipped automobiles (0.44), whereas IP/(BghiP+IP) ratios (0.18, 0.37 and 0.56) are for cars, diesel, and coal combustion, respectively (Bi et al., 2005).

In this study, we found the ratios of IP/BghiP, Bghi/Bep, Flut/(Flut + Pyr), and IP/(IP+BghiP) are 1.23, 1.17, 0.56, and 0.55, respectively. The ratios are closer to those in coal burning emissions than in vehicular exhausts. These results imply that PAH components in Nanjing winter aerosols are mainly derived from coal combustion. The PAH compositions of our study are different from those reported from Sacramento (Kleeman et al., 2008), Los Angeles and London (Finlayson-Pitts and Pitts Jr, 2000), in which BghiP/BeP ratios are 5.6, 3.5 and 1.7, respectively, when vehicular emissions were the major sources for PAHs in these cities. The present PAH concentrations in Nanjing aerosols are lower than those found in a previous study from Nanjing samples collected in 2004 (Table 2) (Wang et al., 2007a) and one-fourth of those collected in

2001 (214 ng m^{-3}) (Yang et al., 2005), indicating the local air quality in Nanjing is improving since 2001.

3.3.5 Hopanes and Steranes

Hopane and sterane isomers are considered as biomarkers of fossil fuel emissions, which belong to the higher boiling fraction of crude oil and are more resistant to degradation than *n*-alkanes. They are abundantly originated from the crude oil and engine oil, and consequently in vehicle exhaust from unburned lubricating oil residues and road dust (Ding et al., 2009). Six hopane compounds were identified in the Nanjing urban samples (Table S1) with higher levels in nighttime (0.13-26.1 ng m^{-3}, ave. 4.16 ng m^{-3}) and lower levels in daytime (0.09-20.8 ng m^{-3}, 3.78 ng m^{-3}) (Figure 2). The concentrations of hopane in the present study are comparable with those from other Chinese cities and Tokyo (0.7-15 ng m^{-3}; 5.5 ng m^{-3}) (Wang et al., 2006). Wang et al. (2009) reported that concentrations of hopanes in the urban samples were 2 orders of magnitude higher than those in the mountain samples whereas hopanes were not detectable in the marine samples.

The diagnostic ratios of hopanes can differentiate their sources (Table 3). The 17α(H)-21β(H)-29-norhopane ($C_{29}\alpha\beta$)/17α(H)-21β(H)-hopane ($C_{30}\alpha\beta$) ratios of 0.59-0.66, 0.42, and 0.58-2.0 are attributable to gasoline, diesel and coal burning emissions, respectively (Rogge et al., 1993a; Oros and Simoneit, 2000). In addition, the ratios of 17α(H)-21β(H)-22S-homohopane/(17α(H)-21β(H)-22S-homohopane + 17α(H)-21β(H)-22R-homohopane) [$C_{31}\alpha\beta S/(C_{31}\alpha\beta S + C_{31}\alpha\beta R)$] ranging from 0.60-0.62, 0.50, and 0.05-0.37 indicate gasoline, diesel and coal burning emissions, respectively (Rogge et al., 1993a; Oros and Simoneit, 2000). We observed that concentration ratios of $C_{29}\alpha\beta/C_{30}\alpha\beta$ and $C_{31}\alpha\beta S/(C_{31}\alpha\beta S+ C_{31}\alpha\beta R)$ in this study are 0.58 and 0.48, respectively, which are near to those in vehicular emissions than coal combustion. Thus,

hopanes in the Nanjing aerosol are predominantly emitted from traffic emissions due to rapidly increasing of automobiles in Chinese mega-cities.

A series of steranes were also identified in the present study. Concentration ranges of total steranes were 1.14-9.16 ng m^{-3} (ave. 2.29 ng m^{-3}) during daytime and 1.09-11.1 ng m^{-3} (2.64 ng m^{-3}) during nighttime. The diurnal distribution patterns of steranes showed remarkable similarity with hopanes. The strong correlation coefficient was also observed between steranes and hopanes ($r = 0.94$, $p<0.001$), indicating their similar emission sources (Figure S3d). It is reasonable because homologues of hopanes and steranes are very stable and have similar atmospheric fates (Ding et al., 2009). In contrast, PAHs showed positive correlations with hopanes and steranes with a lower correlation coefficient ($r = 0.42$, $p<0.001$), indicating their partly similar sources.

3.3.6 Phthalates

Phthalates are common additives widely used as a softener and plasticizers in polyvinylchloride (PVC) and synthetic polymers, respectively. It can be emitted into the atmosphere through the evaporation process due to their weak bonding in the polymer. Phthalates have potential health effect due to their endocrine disrupting and carcinogenic properties (Sidhu et al., 2005). It is necessary to pay attention to phthalates as toxic components in the aerosol particles. However, few studies have reported their atmospheric distribution over China (Fu et al., 2008; Wang et al., 2006, 2007a). Four phthalate esters, i.e., diethyl (DEP), di-iso-butyl (DiBP), di-n-butyl (DnBP), and di-(2-ethylhexyl) (DEHP) phthalates were characterized in this study with total concentrations of 13.9 ng m^{-3} (range, 2.66-40.0 ng m^{-3}) in daytime and 16.3 ng m^{-3} (3.79-51.8 ng m^{-3}) in nighttime (Figure 7a). DnBP (ave. 8.07 ng m^{-3}) is the dominant tracer, followed by DEHP (4.00 ng m^{-3}), DiBP (2.59 ng m^{-3}) and DEP (0.14 ng m^{-3}). The levels of phthalates in this study are 4-20 times lower than those proposed in other

525 Chinese megacities in 2006 (Wang et al., 2006), although comparable than those
526 observed from Paris, France (8.2 ng m^{-3}) (Teil et al., 2006), Sweden (3.7 ng m^{-3})
527 (Thuren and Larsson, 1990), and Texas, USA (2.1 ng m^{-3}) (Weschler, 1984).

528 The evaporation of phthalates can be accelerated under high ambient
529 temperature conditions. The higher values in nighttime than daytime of phthalates in
530 Nanjing aerosol is opposite with the result of Mt. Tai aerosols (Fu et al., 2008) due to
531 the decreased PBLH in nighttime. Moreover, there is no significant difference in
532 temperature between day and night during the campaign in Nanjing (Figure S1).
533 Significant correlations were found between DEP and DiBP ($r = 0.85$, $p<0.001$) as well
534 as DiBP and DnBP ($r = 0.87$, $p<0.001$) (Figures S4a and S4b), suggesting that these
535 compounds are commonly used as plasticizers in China and released in the same way
536 into the atmosphere. It should be noted that the concentration level of phthalates in this
537 study is 1-2 orders of magnitude lower than those found in Nanjing aerosols collected in
538 2004 (ave. 230 ng m^{-3}) (Wang et al., 2007a), suggesting a significant improvement of
539 local air quality in Nanjing regarding plastic emission.

540 **3.3.7 Aromatic acids**

541 We detected benzoic acid and three phthalic acids in the urban aerosols from
542 Nanjing with total concentrations of 6.70 ng m^{-3} (1.53-23.1 ng m^{-3}) in daytime and 8.37
543 ng m^{-3} (1.99-18.5 ng m^{-3}) in nighttime (Figure 7b). These acids can play a significant
544 role to increase the formation of new particles in the atmosphere (Zhang et al., 2004).
545 Benzoic acid ranged from 0.17-0.95 ng m^{-3} (ave. 0.45 ng m^{-3}) in daytime and 0.24-1.22
546 ng m^{-3} (0.54 ng m^{-3}) in nighttime (Table S1), which is 1 and 4 orders of magnitude
547 lower than summertime aerosol of Mt. Tai and wintertime aerosol of tropical India,
548 respectively (Fu et al., 2008, 2010). Benzoic acid is primarily emitted from automobiles

549 (Rogge et al., 1993b; Kawamura et al., 2000) but also been proposed as a secondary
550 component via a photooxidation of several aromatic hydrocarbons (Fu et al., 2010).

551 Total phthalic acids varied from 1.40-21.9 ng m^{-3} (ave. 6.25 ng m^{-3}) during
552 daytime and 1.76-16.8 ng m^{-3} (7.83 ng m^{-3}) during nighttime. Their concentrations are
553 lower than those found during aircraft measurement over China in summer (17±13 ng
554 m^{-3}) (Wang et al., 2007b) but higher than the samples measured from the northwestern
555 Pacific (ave. 1.5 ng m^{-3}) (Simoneit et al., 2004a). The molecular distributions of
556 phthalic acids showed the dominance of terephthalic acid (Figure 7b), which accounted
557 for 82% of total aromatic acids in Nanjing samples. Phthalic acids are SOA products
558 produced from several PAHs (Oliveira et al., 2007; Fine et al., 2004). It is noteworthy
559 that PAHs mostly produce phthalic acids over the North China Plain (Fu et al., 2008).
560 Terephthalic acid can be derived from plastics burning as well (Fu et al., 2010).

561 Aromatic acids showed positive correlations with 4 and 5 rings PAHs ($r = 0.56$,
562 $p<0.001$) and phthalates ($r = 0.71$, $p<0.001$) (Figure S3c), suggesting that they are
563 primarily derived from PAHs. Furthermore, aromatic acids showed significant
564 correlation with oxidation products of polyacids ($r = 0.83$, $p<0.001$) (Figure S4c),
565 indicating the secondary oxidation process is a major source of aromatic acids.
566 However, higher concentrations of aromatic acids in nighttime rather than daytime may
567 not explain photochemical oxidation. We propose two explanations for the high level of
568 SOA products in nighttime. First, SOA products are formed during long-range
569 atmospheric transport that is consistent with aged PAHs in the aerosols as discussed
570 above (section 3.3.4). Second, NOx can play an important role to oxidize PAHs in
571 nighttime when NOx concentration is high (Offenberg et al., 2007; Henze et al., 2008).
572 However, further studies are needed for the justification of NOx influence in the
573 Nanjing atmosphere.

574 **3.3.8 Hydroxy-/polyacids**

575 Glycerol and several polyacids were identified in all the samples from Nanjing
576 (Table S1). Glycerol is a primary product of a metabolic reaction of soil organisms,
577 while polyacids are secondarily produced by photo-oxidation of organic precursors
578 (Simoneit et al., 2004c). Glycerol didn't show significant correlation with polyacids (r =
579 0.21-0.38), implying their different sources (i.e., primary and secondary). Kawamura
580 and Ikushima(1993), and Matsunaga et al. (1999) reported that malic acid is a
581 photooxidation product of succinic acid, which is one of the photooxidation products of
582 biogenic unsaturated fatty acids (BUFAs) in the atmosphere. Moreover, SOA tracers,
583 including malic and tartaric acids are produced by the photochemical oxidation of
584 isoprene (Claeys et al., 2004).

585 The concentration range of glycerol was 0.66-5.99 ng m^{-3} (ave. 2.67 ng m^{-3})
586 during daytime and 0.73-8.72 ng m^{-3} (3.50 ng m^{-3}) during nighttime. Glycerol is a
587 dominant component in this group (Table S1 and Figure7c), which is consistent with
588 the previous report from Nanjing aerosol in 2004-2005, whereas present concentration
589 level is lower than that reported in Nanjing (Wang and Kawamura, 2005).
590 Concentrations ranges of total polyacids were 1.21-23.5 ng m^{-3} (5.1 ng m^{-3}) during
591 daytime and 2.05-11.2 ng m^{-3} (5.80 ng m^{-3}) during nighttime, among which tartaric acid
592 (2.18 ng m^{-3}) was dominant (Figure 7c). Tartaric acid presented a positive correlation
593 with levoglucosan ($r = 0.75$, $p<0.001$) (Figure S2b), suggesting an influence of biomass
594 burning. Significant correlations were found among all polyacids ($r = 0.50$-0.75,
595 $p<0.001$), indicating their similar source or formation pathway. Polyacids showed a
596 strong correlation with WSOC ($r = 0.85$, $p<0.001$) (Figure S4d), indicating their water-
597 soluble and hygroscopic nature and therefore it might influence the CCN activities of
598 aerosol particles. It should be noted that secondary oxidation products are formed

during long-range atmospheric transport, which can explain high values of polyacids in nighttime. This result is consistent with the high WSOC/OC ratio in Nanjing aerosols (see section 3.2) as well as air mass back trajectories (Figure S5).

3.4 Source apportionment of organic aerosols using PMF

Positive matrix factorization (PMF5.0, USEPA) analysis was performed in this study for better understanding the sources of the identified components. It is a statistical source apportionment model widely used to verify underlying covariance among chemical parameters (Paatero and Tapper, 1994; Jaeckels et al., 2007). Detailed information of the PMF model can be found elsewhere (Paatero, 1997; Paatero and Tapper, 1994). PMF model was applied for apportioning ambient PM to motor vehicle and wood combustion emission, SOA, and two-point sources using organic molecular markers (Jaeckels et al., 2007). This model has also been extensively used for identifying source profile and source contribution of PM based elemental and organic markers data (Song et al., 2001; Buzcu et al., 2003; Jaeckels et al., 2007; Jia et al., 2010). The analytical errors estimated for the measured values of chemical species in PMF analysis are 10%. The detected organic compound classes were subjected to source apportionment evaluation to make the classifications of sources using the model. PMF model application resolved 5 source factors based on Q values that contributed to ambient $PM_{2.5}$ in this study. OC, EC and some inorganic ions were also used to investigate possible different sources. We used $PM_{2.5}$ as the sum of total variables during the model convergence. Figure 8 shows composition source profiles for the five factors resolved by PMF analysis, where factor 3 is a dominant source.

Factor 1 is dominated by levoglucosan (69%) followed by fatty alcohol (C_{30}) (56%), arabitol (44%) and *n*-alkane (C_{29}) (34%). Factor 1 is associated with biomass burning because levoglucosan is a specific tracer of biomass burning. Moreover, fatty

624 alcohols, fatty acids, *n*-alkanes, and sugar compounds can also be emitted from biomass
625 burning. Biomass materials, including rice and wheat straws, and cotton stems, are
626 widely used for domestic cooking in rural areas around Nanjing, particularly in the
627 evening. Therefore, particles from biomass burning are abundantly released into the
628 atmosphere and then transported to the Nanjing urban area. This idea is consistent with
629 high loadings of biomass burning tracers during nighttime.

630 Factor 2 is enriched with nss-Ca^{2+} (75 %), suggesting that the component is
631 associated with soil dust because it is a specific tracer of soil dust (Athanasopoulou et
632 al., 2010; Brahney et al., 2013). Many infrastructures of the urban area are constructing
633 in China, which can produce dust particles largely and emit into the atmosphere. Factor
634 3 is attributed to secondary oxidation products because of the dominant species in this
635 source profile is malic acid (69%). Malic acid is a secondary oxidation product as
636 described above (see section 3.3.8).

637 Factor 4 was abundantly loaded by fluoranthene (representative PAH) (79%),
638 $C_{30}\alpha\beta$ (representative hopane) (64%) and C_{29} (representative *n*-alkane) (50%), implying
639 their origination from the fossil fuel combustion. It should be noted that *n*-alkanes also
640 showed a loading in factor 1, suggesting that *n*-alkanes are partly associated with
641 biomass burning. PAHs can be emitted from fossil fuel combustion and biomass
642 burning activities. However, we observed that PAHs are mainly derived from fossil fuel
643 combustion in Nanjing (see section 3.3.4). Furthermore, *n*-alkanes can be originated
644 from fossil fuel combustion and higher plant waxes, whereas fossil fuel was the
645 dominant source for *n*-alkanes in Nanjing aerosols (see section 3.3.1). Hopanes are
646 emitted from the vehicular exhaust as well as coal burning. Low-quality coals are
647 extensively used in urban and rural areas in China for cooking and house heating. Many
648 power plants in Chinese cities also used a large amount of coal for producing energy.

649 Running vehicles have also increased severely in China, which can emit hopanes in the
650 atmosphere. Factor 5 is dominated by di-(2-ethylhexyl) phthalate (DEHP) (63%)
651 followed by terephthalic acid (35%), which should be associated with plastic burning.
652 Terephthalic acid is a secondary oxidation product and also can be emitted from the
653 open burning of plastics as discussed above.

654 PMF results can be further utilized to calculate the relative contributions of
655 sources to the amount of ambient OC or $PM_{2.5}$ using a multiple linear regression
656 between the isolated factor strengths and measured OC or $PM_{2.5}$ (Song et al., 2001).
657 Results of this analysis are presented in Figure 9 whereas source contributions were
658 calculated to $PM_{2.5}$. Fossil fuel combustion was the dominant source (28.7%)
659 considering the primary source, followed by emissions of biomass burning (17.1%), soil
660 dust (14.5%), and plastic burning (6.83%) during this study period. However, secondary
661 oxidation products showed the highest contribution (32.9%) to $PM_{2.5}$ in Nanjing
662 probably due to long-range atmospheric transport. These results indicate that fossil fuel
663 combustion is an important contributor to Nanjing aerosol during winter. Wang and
664 Kawamura (2005) reported that fossil fuel combustion (52%) was the largest
665 contributor to total organics followed by biomass burning (14%) and SOA (10%) from
666 Nanjing, whereas coal combustion was found to contribute to $PM_{2.1}$ by 39.5% in 2010
667 in Nanjing (Chen et al., 2015). Gao et al. (2013) pointed out that coal combustion was
668 the dominant (58%) contributor to $PM_{2.5}$ followed by biomass burning (31%), and
669 vehicular emissions (11%) in the Pearl River Delta region (two urban, two suburban
670 and two rural sites) while sample was collected in 2009. The comparison of current
671 results with previous studies implies that the contribution of fossil fuel combustion and
672 biomass burning emission in China decreased significantly in the past decade.

673 However, pollution levels in China are still severe compared to those in the National
674 and WHO standards as discussed above (section 1).

675 **4. Summary and Conclusions**

676 We collected $PM_{2.5}$ aerosol samples during winter from Nanjing, an urban area
677 located in east China in 2014 to 2015. Twelve organic compound classes were
678 identified in the aerosol samples with *n*-alkanes as the dominant compound class,
679 followed by fatty acids, PAHs, anhydro-sugars, fatty alcohols, and phthalate esters. The
680 concentrations of organic compounds were slightly higher at night samples than day
681 samples because of the lower PBLH and more emissions from heavy-duty trucks as
682 well as coal and biomass burning in nighttime.

683 The molecular signature of *n*-alkanes with a weak odd-carbon number
684 predominance and maxima of C_{29} (ave. CPI: 1.18) implies their significant emission
685 from fossil fuels combustion. On the contrary, microbial and plant waxes are the major
686 source of fatty acids and fatty alcohols in this study. Fatty alcohols are also significantly
687 emitted from biomass burning. The biomass burning tracer, levoglucosan was the
688 dominant species among the detected compounds. Levoglucosan and other biomass
689 burning tracers are mainly originated from house cooking and heating during study
690 period. Concentrations of secondary oxidation products, including aromatic acids and
691 polyacids, maximized during nighttime possibly because of the influence of NO_x or
692 long-range atmospheric transport.

693 The diagnostic ratios of the tracer compounds suggest that coal burning is the
694 major source of PAHs while hopanes are abundantly emitted from traffic emissions
695 over Nanjing atmosphere. PMF analysis demonstrated that fossil fuel combustion is an
696 important source (28.7%) in Nanjing winter aerosols. The concentrations of organic
697 tracers in this study are lower than previously reported Nanjing aerosols collected in

2004-2005. Air quality in Nanjing may have been improved for last decade. However, fossil fuel combustion emissions have not been decreased satisfactorily and still control the compositions of wintertime OAs in Nanjing atmosphere.

Acknowledgements

We acknowledge the Natural Scientific Foundation of China (Grant No. 91643109 and 41603104) and Japan Society for the Promotion of Science (Grant No. 24221001) for financial support.

References

Albrecht, B. A.: Aerosols, Cloud Microphysics, and Fractional Cloudiness, Science, 245(4923), 1227–1230. https://doi.org/10.1126/science.245.4923.1227, 1989.

Asa-Awuku, A., Moore, R. H., Nenes, A., Bahreini, R., Holloway, J. S., Brock, C. A., Middlebrook, A. M., Ryerson, T. B., Jimenez, J. L., Decarlo, P. F., Hecobian, A., Weber, R. J., Stickel, R., Tanner, D. J., and Huey, L. G.: Airborne cloud condensation nuclei measurements during the 2006 Texas Air Quality Study, J. Geophys. Res.- Atmos., 116(11), doi:10.1029/2010JD014874, 2011.

Athanasopoulou, E., Tombrou, M.,Russell, A. G.. Karanasiou, A., Eleftheriadis, K., and Dandou, A.: Implementation of road and soil dust emission parameterizations in the aerosol model CAMx: Applications over the greater Athens urban area affected by natural sources, J. Geophys. Res., 115(D17301), doi:10.1029/2009JD013207., 2010.

Bi, X., Sheng, G., Peng, P., Chen, Y., Zhang, Z., and Fu, J.: Distribution of particulate- and vapor-phase *n*-alkanes and polycyclic aromatic hydrocarbons in urban atmosphere of Guangzhou, China, Atmos. Environ., 37(2), 289–298, 2003.

Bi, X., Sheng, G., Peng, P., Chen, Y., and Fu, J.: Size distribution of n-alkanes and polycyclic aromatic hydrocarbons (PAHs) in urban and rural atmospheres of Guangzhou, China, Atmos. Environ., 39(3), 477–487,, 2005.

Boreddy, S. K. R., Haque, M. M., and Kawamura, K.: Long-term (2001-2012) trends of carbonaceous aerosols from a remote island in the western North Pacific: An outflow region of Asian pollutants, Atmos. Chem. Phys., 18(2), 1291–1306, doi:10.5194/acp-18-1291-2018, 2018.

Brahney, J., Ballantyne, A. P., Sievers, C., and Neff, J. C.: Increasing Ca^{2+} deposition in the western US: The role of mineral aerosols, Aeolian Res., 10, 77–87, 2013.

Buzcu, B., Fraser, M. P., Kulkarni, P., and Chellam, S.: Source identification and apportionment of fine particulate matter in Houston, TX, using positive matrix factorization, Environ. Eng. Sci., 20(6), 533–545, 2003.

Chang, Y., Zhang, Y., Tian, C., Zhang, S., Ma, X., Cao, F., Liu, X., Zhang, W., Kuhn, T., and Lehmann, M. F.: Nitrogen isotope fractionation during gas-particle conversion of NOx to NO_3^- in the atmosphere – implications for isotope-based NOx source apportionment, Atmos. Chem. Phys., 18, 11647-11661, https:// doi.org/ 10.5194/acp-18-11647-2018, 2018.

739 Chen, P., Wang, T., Hu, X., and Xie, M: Chemical Mass Balance Source
740 Apportionment of Size-Fractionated Particulate Matter in Nanjing, China, Aerosol
741 and Air Quality Research, 15, 1855–1867, 2015.
742 Chung, S. H., and Seinfeld, J. H.: Global distribution and climate forcing of
743 carbonaceous aerosols, J. Geophys. Res.- Atmos., 107((D19)), 4407,
744 doi:10.1029/2001JD001397, 2002.
745 Chung, C. E., Ramanathanb, V., and Decremer, D.: Observationally constrained
746 estimates of carbonaceous aerosol radiative forcing, PNAS, 109, 11624–11629; 109,
747 11624–11629, doi:10.1073/pnas.1203707109, 2012.
748 Claeys, M., Graham, B., Vas, G., Wang, W., Vermeylen, R., Pashynska, V., Cafmeyer,
749 J., Guyon, P., Andreae, M. O., Artaxo, P., and Maenhaut, W.: Formation of
750 secondary organic aerosols through photooxidation of isoprene, Science (80-.)..,
751 303(5661), 1173–1176, 2004.
752 Cooke, W. F., Liousse, C., Cachier, H., and Feichter, J.: Construction of a 1 degrees x 1
753 degrees fossil fuel emission data set for carbonaceous aerosol and implementation
754 and radiative impact in the ECHAM4 model, J. Geophys. Res.- Atmos., 104(D18),
755 22137–22162, 1999.
756 Ding, X., Wang, X. M., Xie, Z. Q., Xiang, C. H., Mai, B. X., Sun, L. G., Zheng, M.,
757 Sheng, G. Y., Fu, J. M., and Pöschl, U.: Atmospheric polycyclic aromatic
758 hydrocarbons observed over the North Pacific Ocean and the Arctic area: Spatial
759 distribution and source identification, Atmos. Environ., 41, 2061–2072, 2007.
760 Ding, L. C., Fu, K.,Wang, D. K. W.,Dann, T., andAustin, C. C.: A new direct thermal
761 desorption-GC/MS method: Organic speciation of ambient particulate matter
762 collected in Golden, BC, Atmos. Environ., 43, 4894–4902, 2009.
763 Ding, X., Wang, X., Xie, Z., Zhang, Z., and Sun, L.: Impacts of siberian biomass
764 burning on organic aerosols over the north pacific ocean and the arctic: Primary and
765 secondary organic tracers, Environ. Sci. Technol., 47(7), 3149–3157, 2013.
766 Dusek, U., Frank, G. P., Hildebrandt, L., Curtius, J., Schneider, J., Walter, S., Chand,
767 D., Drewnick, F., Hings, S., Jung, D., Borrmann, S., and Andreae, M. O.: Size
768 matters more than chemistry for cloud-nucleating ability of aerosol particles, Science
769 (80-.)., 312(5778), 1375–1378, 2006.
770 Elbert, W., Taylor, P. E., Andreae, M. O., and Poschl, U.: Contribution of fungi to
771 primary biogenic aerosols in the atmosphere: wet and dry discharged spores,
772 carbohydrates, and inorganic ions, Atmos. Chem. Phys., 7, 4569–4588, 2007.
773 Finlayson-Pitts, B. J., and Pitts Jr, J. N.: Chemistry of the Upper and Lower
774 Atmosphere, Academic Press, San Diego, 2000.
775 Fine, P. M., Chakrabarti, B., Krudysz, M., Schauer, J. J., and Sioutas, C.: Diurnal
776 variations of individual organic compound constituents of ultrafine and accumulation
777 mode particulate matter in the Los Angeles basin, Environ. Sci. Technol., 38(5),
778 1296–1304, 2004.
779 Fu, P. Q., Kawamura, K., Okuzawa, K., Aggarwal, S. G., Wang, G., Kanaya, Y., and
780 Wang, Z.: Organic molecular compositions and temporal variations of summertime
781 mountain aerosols over Mt. Tai, North China Plain, J. Geophys. Res.-Atmos., 113,
782 D1910, doi:10.1029/2008JD009900, 2008.
783 Fu, P. Q., Kawamura, K., and Barrie, L. A.: Photochemical and other sources of organic
784 compounds in the Canadian high Arctic aerosol pollution during winter-spring,
785 Environ. Sci. Technol., 43(2), 286–292, 2009.
786 Fu, P. Q., Kawamura, K., Pavuluri, C. M., Swaminathan, T., and Chen, J.: Molecular
787 characterization of urban organic aerosol in tropical India: contributions of primary
788 emissions and secondary photooxidation, Atmos. Chem. Phys., 10(6), 2663–2689,
789 2010.
790 Gao, B., Guo, H., Wang, X. M., Zhao, X. Y., Ling, Z. H., and Zhang, Z.: Tracer-based

source apportionment of polycyclic aromatic hydrocarbons in $PM_{2.5}$ in Guangzhou southern China, using positive matrix factorization (PMF). Environ. Sci. Poll. Res. Int., 20, 2398–2409, 2013.
Graham, B., Guyon, P., Taylor, P. E., Artaxo, P., Maenhaut, W., Glovsky, M. M., Flagan, R. C., and Andreae, M. O.: Organic compounds present in the natural Amazonian aerosol: Characterization by gas chromatography-mass spectrometry, J. Geophys. Res.-Atmos., 108, D24, 4766, doi:10.1029/2003JD003990, 2003.
Grimmer, G., Jacob, J., and Noujack, K. W.: Profile of the polycyclic aromatic hydrocarbons from lubricating oils. Inventory by GC/MS-PAH in environmental materials, part 1., Fresenius Zeitschrift fur Anal. Chemie, 314, 13–19., 1983.
Guo, Z. G., Sheng, L. F., Feng, J. L., and Fang, M.: Seasonal variation of solvent extractable organic compounds in the aerosols in Qingdao, China, Atmos. Environ., 37(13), 1825–1834, doi:10.1016/S1352-2310(03)00064-5, 2003.
Haque, M. M., Kawamura, K., and Kim, Y.: Seasonal variations of biogenic secondary organic aerosol tracers in ambient aerosols from Alaska, Atmos. Environ., 130, 95–104, doi:10.1016/j.atmosenv.2015.09.075, 2016.
Hays, M. D., Fine, P. M., Geron, C. D., Kleeman, M. J., and Gullett, B. K.: Open burning of agricultural biomass: Physical and chemical properties of particle-phase emissions, Atmos. Environ., 39(36), 6747–6764, 2005.
He, K., Zhao, Q., Ma, Y., Duan, F., Yang, F., Shi, Z., and Chen, G: Spatial and seasonal variability of $PM_{2.5}$ acidity at two Chinese megacities: insights into the formation of secondary inorganic aerosols, Atmos. Chem. Phys., 12, 1377–1395, doi:10.5194/acp-12-1377-2012, 2012.
Henze, D. K., Seinfeld, J. H., Ng, N. L., Kroll, J. H., Fu, T. M., Jacob, D. J., and Heald, C. L.: Global modeling of secondary organic aerosol formation from aromatic hydrocarbons: high- vs. low-yield pathways, Atmos. Chem. Phys., 8(9), 2405–2420, doi:10.5194/acp-8-2405-2008, 2008.
Huebert, B. J., Bates, T., Russell, P. B., Shi, G. Y., Kim, Y. J., Kawamura, K., Carmichael, G., and Nakajima, T.: An overview of ACE-Asia: Strategies for quantifying the relationships between Asian aerosols and their climatic impacts, J. Geophys. Res.-Atmos., 108(D23), doi:10.1029/2003JD003550, 2003.
Jacobson, M. Z.: Global direct radiative forcing due to multicomponent anthropogenic and natural aerosols, J. Geophys. Res.- Atmos., 106(D2), 1551–1568, doi:10.1029/2000JD900514, 2001.
Jaeckels, J. M., Bae, M. S., and Schauer, J. J.: Positive matrix factorization (PMF) analysis of molecular marker measurements to quantify the sources of organic aerosols, Environ. Sci. Technol., 41(16), 5763–5769, 2007.
Jia, Y. L., Clements, A. L., and Fraser, M. P.: Saccharide composition in atmospheric particulate matter in the southwest US and estimates of source contributions, J. Aerosol Sci., 41(1), 62–73, doi:10.1016/j.jaerosci.2009.08.005, 2010.
Kanakidou, M., Seinfeld, J. H., Pandis, S. N., Barnes, I., Dentener, F. J., Facchini, M. C., Van Dingenen, R., Ervens, B., Nenes, A., Nielsen, C. J., Swietlicki, E., Putaud, J. P., Balkanski, Y., Fuzzi, S., Horth, J., Moortgat, G. K., Winterhalter, R., Myhre, C. E. L., Tsigaridis, K., Vignati, E., Stephanou, E. G., and Wilson, J.: Organic aerosol and global climate modelling: a review, Atmos. Chem. Phys., 5, 1053–1123, 2005.
Kawamura, K., and Gagosian, R. B.: Implications of ω-oxocarboxylic acids in the remote marine atmosphere for photo-oxidation of unsaturated fatty acids, Nature, 325, 330–332, 1987.
Kawamura, K., and Ikushima, K.: Seasonal changes in the distribution of dicarboxylic acids in the urban atmosphere, Environ. Sci. Technol., 27(10), 2227–2235, 1993.
Kawamura, K., Kosaka, M., and Sempéré, R.: Distributions and seasonal changes of hydrocarbons in urban aerosols and rainwaters, Chikyukagaku (Geochemistry), 29, 1–15, 1995.
Kawamura, K., Steinberg, S., and Kaplan, I. R.: Homologous series of C_1-C_{10} monocarboxylic acids and C_1-C_6 carbonyls in Los Angeles air and motor vehicle exhausts, Atmos. Environ., 34(24), 4175–4191, 2000.
Kawamura, K., Ishimura, Y., and Yamazaki, K.: Four years' observations of terrestrial

lipid class compounds in marine aerosols from the western North Pacific, Glob. Biogeochem. Cycles,. 17, 1003(1), doi:10.1029/2001GB001810, 2003.
Kendrick, C. M., Koonce, P., and George, L. A.: Diurnal and seasonal variations of NO, $NO_2$and $PM_{2.5}$ mass as a function of traffic volumes alongside an urban arterial, Atmos. Environ., 122, 133–141, doi:10.1016/j.atmosenv.2015.09.019, 2015.
Kerimray, A., Luis, R.-S., Torkmahalleh, M. A., Hopke, P. K., Gallachóir, B. P. Ó.: Coal use for residential heating: Patterns, health implications and lessons learned, Ener. Sus. Devlop., 40, 19–30, 2017.
Kleeman, M. J., Riddle, S. G., and Jakober, C. A.: Size distribution of particle-phase molecular markers during a severe winter pollution episode, Environ. Sci. Technol., 42, 6469–6475, 2008.
Kolattukudy, P. E.: Chemistry and Biochemistry of Natural Waxes, Elsevier, New York., 1976.
Kunwar, B., and Kawamura, K.: One-year observations of carbonaceous and nitrogenous components and major ions in the aerosols from subtropical Okinawa Island, an outflow region of Asian dusts, Atmos. Chem. Phys., 14, 1819–1836, doi:https://doi.org/10.5194/acp-14-1819-2014, 2014.
Li, M., Zhang, Q., Kurokawa, J.-I., Woo, J-H., He, K., Lu, Z., Ohara, T., Song, Y.,. Streets, D. G., Carmichael, G. R., Cheng, Y., Hong, C., Huo, H., Jiang, X., Kang, S., Liu, F., Su, H., and Zheng, B: MIX: a mosaic Asian anthropogenic emission inventory under the international collaboration framework of the MICS-Asia and HTAP, Atmos. Chem. Phys., 17, 935–963, 2017.
Liu, J., Han, Y., Tang, X., Zhu, J., and Zhu, T: Estimating adult mortality attributable to $PM_{2.5}$ exposure in China with assimilated $PM_{2.5}$ concentrations based on a ground monitoring network. Sci. Total Environ., 568, 1253–1262. doi:10.1016/j.scitotenv. 2016.05.165, 2016.
Lohmann, U., Feichter, J., Penner, J., and Leaitch, R.: Indirect effect of sulfate and carbonaceous aerosols: A mechanistic treatment, J. Geophys. Res.- Atmos., 105(D10), 12193–12206, doi:10.1029/1999JD901199, 2000.
Matsunaga, S., Kawamura, K., Nakatsuka, T., and Ohkouchi, N.: Preliminary study on laboratory photochemical formation of low molecular weight dicarboxylic acids from unsaturated fatty acid (oleic acid), Res. Org. Geochem., 14, 19–25, 1999.
Ma, Z., Hu, X., Sayer, A. M., Levy, R., Zhang, Q., Xue, Y., Tong, S., Bi, J., Huang, L., Liu, Y.: Satellite-based spatiotemporal trends in $PM_{2.5}$ concentrations: China, 2004–2013, Environ. Health Perspect., 124, 184–192, http://dx.doi.org/10.1289/ ehp.1409481, 2016.
Medeiros, P. M., Conte, M. H., Weber, J. C. and Simoneit, B. R. T.: Sugars as source indicators of biogenic organic carbon in aerosols collected above the Howland Experimental Forest, Maine, Atmos. Environ., 40(9), 1694–1705, 2006.
Medeiros, P. M., and Simoneit, B. R. T.: Source profiles of organic compounds emitted upon combustion of green vegetation from temperate climate forests, Environ. Sci. Technol., 42(22), 8310–8316, 2008.
Mochida, M., Kitamori, Y., Kawamura, K., Nojiri, Y., and Suzuki, K.: Fatty acids in the marine atmosphere: Factors governing their concentrations and evaluation of organic films on sea-salt particles, J. Geophys. Res.-Atmos., 107, D17, 4325, doi:10.1029/2001JD001278, 2002.
Mochida, M., Kawamura, K.,Fu, P., and Takemura,T.: Seasonal variation of levoglucosan in aerosols over the western North Pacific and its assessment as a biomass-burning tracer, Atmos. Environ., 44, 3511-3518, 2010.
Mochizuki, T., Miyazaki, Y., Ono, K., Wada, R., Takahashi, Y., Saigusa, N., Kawamura, K., and Tani, A.: Emissions of biogenic volatile organic compounds and subsequent formation of secondary organic aerosols in a Larix kaempferi forest, Atmos. Chem. Phys., 15(20), 12029–12041, doi:10.5194/acp-15-12029-2015, 2015.
O'Dowd, C. D., Facchini, M. C., Cavalli, F., Ceburnis, D., Mircea, M., Decesari, S.,

902 Fuzzi, S., Yoon, Y. J., and Putaud, J. P.: Biogenically driven organic contribution to
903 marine aerosol, Nature, 431, 676–680, 2004.
904 Offenberg, J., Lewis, C., Lewandowski, M., Jaoui, M.,Kleindienst, T. E., and Edney, E.
905 O.: Contributions of Toluene and α-Pinene to SOA formed in an irradiated toluene/α-
906 Pinene/NOx/air mixture: Comparison of results using ^{14}C content and SOA organic
907 tracer methods, Environ. Sci. Tec., 41, 3972–3976, 2007.
908 Ohura, T., Amagai, T., Fusaya, M., and Matsushita, H.: Polycyclic Aromatic
909 Hydrocarbons in Indoor and Outdoor Environments and Factors Affecting Their
910 Concentrations, Environ. Sci. Technol., 38(1), 77–83, doi:10.1021/es030512o, 2004.
911 Oliveira, C., Pio, C., Alves, C., Evtyugina, M., Santos, P., Goncalves, V., Nunes, T.,
912 Silvestre, A. J. D., Palmgren, F., Wahlin, P., and Harrad, S.: Seasonal distribution of
913 polar organic compounds in the urban atmosphere of two large cities from the North
914 and South of Europe, Atmos. Environ., 41, 5555–5570, 2007.
915 Oros, D. R., and Simoneit, B. R. T.: Identification and emission rates of molecular
916 tracers in coal smoke particulate matter, Fuel, 79(5), 515–536, doi:10.1016/S0016-
917 2361(99)00153-2, 2000.
918 Paatero, J.: Least squares formulation of robustnon-negative factor analysis., Chemom.
919 Andin., 37(1), 23–35, 1997.
920 Paatero, P., and Tapper, U.: Positive Matrix Factorization - A Nonnegative Factor
921 Model With Optimal Utilization of Error-Estimates of Data Values, Environmetrics,
922 5(2), 111–126, doi:10.1002/env.3170050203, 1994.
923 Pani, S. K., Lee, C. T., Chou, C. C. K., Shimada, K., Hatakeyama, S., Takami, A.,
924 Wang, S. H., and Lin, N. H.: Chemical Characterization of Wintertime Aerosols over
925 Islands and Mountains in East Asia: Impacts of the Continental Asian Outflow,
926 Aerosol Air Qual. Res., 17, 3006–3036, 2017.
927 Pope, C. A., Ezzati, M., and Dockery, D. W.: Fine-particulate air pollution and life
928 expectancy in the United States, N. Engl. J. Med., 360, 376–386, 2009.
929 Ram, K., Sarin, M. M., and Hegde, P.: Atmospheric abundances of primary and
930 secondary carbonaceous species at two high-altitude sites in India: Sources and
931 temporal variability, Atmos. Environ., 42, 6785-6796, 2008.
932 Ramírez, N., Cuadras, A., Rovira, E., Marc e, R. M., and Borrull, F.: Risk assessment
933 related to atmospheric polycyclic aromatic hydrocarbons in gas and particle phases
934 near industrial sites, Environ. Heal. Perspect., 119(8), 1110–1116, 2011.
935 Riipinen, I., Yli-Juuti, T., Pierce, J. R., Petaja, T., Worsnop, D. R., Kulmala, M., and
936 Donahue, N. M.: The contribution of organics to atmospheric nanoparticle growth,
937 Nat. Geosci., 5, 453–458., 2012.
938 Rogge, W. F., Mazurek, M. A., Hildemann, L. M., Cass, G. R., and Simoneit, B. R. T.:
939 Quantification of urban organic aerosols at a molecular level: Identification,
940 abundance and seasonal variation, Atmos. Environ., Part A, 27(8), 1309–1330,
941 1993a.
942 Rogge, W. F., Hildemann, L. M., Mazurek, M. A., Cass, G. R., and Simoneit, B. R. T.:
943 Sources of Fine Organic Aerosol. 2. Noncatalyst and Catalyst-Equipped Automobiles
944 and Heavy-Duty Diesel Trucks, Environ. Sci. Technol., 27(4), 636–651,
945 doi:10.1021/es00041a007, 1993b.
946 Saarikoski, S., Timonen, H., Saarnio, K.,Aurela, M., Jrvi, L., Keronen, P., Kerminen, V.
947 M., and Hillamo,R.:Sources of organic carbon in fine particulate matter in northern
948 European urban air, Atmos. Chem. Phys., 8, 6281-6295, 2008.
949 Salma, I., Németh, Z., Weidinger, T., Maenhaut, W.,Claeys, M., Molnár, M., Major, I.,
950 Ajtai, T., Utry, N., and Bozóki, Z. : Source apportionment of carbonaceous chemical
951 species to fossil fuel combustion, biomass burning and biogenic emissions by a

coupled radiocarbon–levoglucosan marker method, Atmos. Chem. Phys., (17), 13767–13781, 2017.
Sandradewi, J., Prevot, A. S. H., Weingartner, E., Schmidhauser, R., Gysel, M., and Baltensperger, U.: A study of wood burning and traffic aerosols in an Alpine valley using a multi-wavelength Aethalometer, Atmos. Environ., 42, 101-112, 2008.
Seinfeld, J. H., and Pandis, S. N.: Atmospheric Chemistry and Physics: From Air Pollution to Climate Change, John Wiley & Sons, New York, 2nd edition, 1232 pp., ISBN-13: 978-0-471-72018-8, 2006.
Shen, G. F., Yuan, S. Y., Xie, Y., Xia, S. J., Li L., Yao, Y. K., Qiao, Y. Z., Zhang, J., Zhao, Q. Y., Ding, A. J., Li, B., and Wu, H. S: Ambient levels and temporal variations of PM2.5 and PM10 at a residential site in the mega-city, Nanjing, in the western Yangtze River Delta, China, J. Environ. Sci. Health, Part A 49, 171–178, 2014.
Sidhu, S., Gullett, B., Striebich, R., Klosterman, J., Contreras, J., and DeVito, M.: Endocrine disrupting chemical emissions from combustion sources: diesel particulate emissions and domestic waste open burn emissions, Atmos. Environ., 39(5), 801–811, 2005.
Simoneit, B. R. T.: The organic chemistry of marine sediments. In Chemical Oceanography, Riley J. P., Chester, R., Eds.; Academic Press:, New York., 1978.
Simoneit, B. R. T., Cardoso, J. N., and Robinson, N.: An assessment of terrestrial higher molecular weight lipid compounds in aerosol particulate matter over the south Atlantic from about 30-70^{o} S, Chemosphere, 23(4), 447–465, 1991a.
Simoneit, B. R. T., Sheng, G. Y., Chen, X. J., Fu, J. M., Zhang, J., and Xu, Y. P.: Molecular marker study of extractable organic-matter in aerosols from urban areas of China, Atmos. Environ., Part A, 25(10), 2111–2129, 1991b.
Simoneit, B. R. T., Schauer, J. J., Nolte, C. G., Oros, D. R., Elias, V. O., Fraser, M. P., Rogge, W. F., and Cass, G. R.: Levoglucosan, a tracer for cellulose in biomass burning and atmospheric particles, Atmos. Environ., 33(2), 173–182, doi:10.1016/S1352-2310(98)00145-9, 1999.
Simoneit, B. R. T.: Biomass burning-a review of organic tracers for smoke from incomplete combustion, Appl. Geochem., 17, 129–162, 2002.
Simoneit, B. R. T., Elias, V. O., Kobayashi, M., Kawamura, K., Rushdi, A. I., Medeiros, P. M., Rogge, W. F., and Didyk, B. M.: Sugars-dominant water-soluble organic compounds in soils and characterization as tracers in atmospheric particulate matter, Environ. Sci. Technol., 38(22), 5939–5949, 2004a.
Simoneit, B. R. T., Kobayashi, M., Mochida, M., Kawamura, K., and Huebert, B. J.: Aerosol particles collected on aircraft flights over the northwestern Pacific region during the ACE-Asia campaign: Composition and major sources of the organic compounds, J. Geophys. Res.- Atmos., 109, D19S0, doi:10.1029/2004JD004565, 2004b.
Simoneit, B. R. T., Kobayashi, M., Mochida, M., Kawamura, K., Lee, M., Lim, H. J., Turpin, B. J., and Komazaki, Y.: Composition and major sources of organic compounds of aerosol particulate matter sampled during the ACE-Asia campaign, J. Geophys. Res.- Atmos., 109, D19S1, doi:10.1029/2004JD004598, 2004c.
Song, X. H., Polissar, A. V., and Hopke, P. K.: Sources of fine particle composition in the northeastern US, Atmos. Environ.,35(31), 5277–5286, 2001.
Stohl, A., Berg, T., Burkhart, J. F., Fjæraa, A. M., Forster, C., Herber, A., Hov Lunder, C., McMillan, W. W., Oltmans, S., Shiobara, M., Simpson, D., Solberg, S., Stebel, K., Str¨om, J., Tørseth, K., Treffeisen, R., Virkkunen, K., and Yttri, K. E.: Arctic

smoke - record high air pollution levels in the European Arctic due to agricultural fires in Eastern Europe in spring 2006, Atmos. Chem. Phys., 7, 511–534, 2007.
Teil, M. J., Blanchard, M., and Chevreuil, M.: Atmospheric fate of phthalate esters in an urban area (Paris—France), Sci. Total Environ., 354, 212–223, 2006.
Thuren, A., and Larsson, P.: Phthalate esters in the Swedish atmosphere, Environ. Sci. Technol., 24, 554–559, 1990.
Twomey, S.: The Influence of Pollution on the Shortwave Albedo of Clouds, J. Atmos. Sci., 34(7), 1149–1152, 1977.
Wang, G., Niu, S., Liu, C., and Wang, L.: Identification of dicarboxylic acids and aldehydes of PM_{10} and $PM_{2.5}$ aerosols in Nanjing, China, Atmos. Environ., 36(12), 1941–1950, doi:10.1016/S1352-2310(02)00180-2, 2002a.
Wang, G., Huang, L., Gao, S., Gao, S., and Wang, L.: Measurements of PM_{10} and $PM_{2.5}$ in urban area of Nanjing, China and the assessment of pulmonary deposition of particle mass, Chemosphere, 48(7), 689–695, doi:10.1016/S0045-6535(02)00197-2, 2002b.
Wang, G., and Kawamura, K.: Molecular characteristics of urban organic aerosols from Nanjing: A case study of a mega-city in China, Environ. Sci. Technol., 39(19), 7430–7438, 2005.
Wang, G., Kawamura, K., Lee, S., Ho, K. F., and Cao, J. J.: Molecular, seasonal, and spatial distributions of organic aerosols from fourteen Chinese cities, Environ. Sci. Technol., 40(15), 4619–4625, 2006.
Wang, G. H., Kawamura, K., Zhao, X., Li, Q. G., Dai, Z. X., and Niu, H. Y.: Identification, abundance and seasonal variation of anthropogenic organic aerosols from a mega-city in China, Atmos. Environ., 41(2), 407–416, doi:Doi 10.1016/J.Atmosenv.2006.07.033, 2007a.
Wang, G., Kawamura, K., Hatakeyama, S., Takami, A., Li, H., and Wang, W.: Aircraft measurement of organic aerosols over China, Environ. Sci. Technol., 41(9), 3115–3120, doi:10.1021/es062601h, 2007b.
Wang, G., Kawamura, K., Xie, M., Hu, S., Gao, S., Cao, J., An, Z., and Wang, Z.: Size-distributions of *n*-alkanes, PAHs and hopanes and their sources in the urban, mountain and marine atmospheres over East Asia, Atmos. Chem. Phys., 9(22), 8869–8882, 2009.
Wang, S., Xing, J., Jang, C., Zhu, Y., Full, J. S., and Hao, J.: Impact Assessment of Ammonia Emissions on Inorganic Aerosols in East China Using Response Surface Modeling Technique, Environ. Sci. Technol., 45 (21), 9293–9300, 2011.
Weschler, C. J.: Indoor–outdoor relationships for non-polar organic constituents of aerosol particles, Environ. Sci. Technol., 18, 648–652, 1984.
Xiao, Q., Ma, Z., Li, S., and Liu, Y.: The Impact of Winter Heating on Air Pollution in China, PLoS ONE 10(1): e0117311. doi:10.1371/journal. pone.0117311, 2015.
Yang, H., Yu, J. Z., Ho, S. S. H., Xu, J. H., Wu, W. S., Wan, C. H., Wang, X. D., Wang, X. R., and Wang, L. S.: The chemical composition of inorganic and carbonaceous materials in $PM_{2.5}$ in Nanjing, China, Atmos. Environ., 39(20), 3735–3749, 2005.
Yao, X., Lau, A. P. S., Fang, M., Chan, C. K., and Hu, M.: Size distributions and formation of ionic species in atmospheric particulate pollutants in Beijing, China: 2 - Dicarboxylic acids, Atmos. Environ., 37(21), 3001–3007, doi:10.1016/S1352-2310(03)00256-5, 2003.
Yttri, K. E., Dye, C., and Kiss, G.: Ambient aerosol concentrations of sugars and sugar-alcohols at four different sites in Norway, Atmos. Chem. Phys., 7, 4267–4279, 2007.
Zhang, R. Y., Suh, I., Zhao, J., Zhang, D., Fortner, E. C., Tie, X. X., Molina, L. T., and

Molina, M. J.: Atmospheric new particle formation enhanced by organic acids, Science (80-.)., 304(5676), 1487–1490, 2004.

Zhang, Q. J., Beekmann, M., Freney, E., Sellegri, K., Pichon, J. M., Schwarzenboeck, A., Colomb, A., Bourrianne, T., Michoud, V., and Borbon, A.: Formation of secondary organic aerosol in the Paris pollution plume and its impact on surrounding regions, Atmos. Chem. Phys., 15(24), 13973–13992, doi:10.5194/acp-15-13973-2015, 2015.

Zhang, Y., and Cao, F.: Fine particulate matter ($PM_{2.5}$) in China at a city level, Sci. Rep., 2015 DOI: 10.1038/srep14884.

Zhang, Y.-L., and Kawamura, K.: New directions: Need for better understanding of source and formation process of phthalic acid in aerosols as inferred from aircraft observations over China, Atmos. Environ., 140, 147–149, 2016.

Zheng, B., Zhang, Q., Zhang, Y., He, K. B., Wang, K., Zheng, G. J., Duan, F. K., Ma, Y. L., and Kimoto, T.: Heterogeneous chemistry: a mechanism missing in current models to explain secondary inorganic aerosol formation during the January 2013 haze episode in North China, Atmos. Chem. Phys., 15, 2031–2049, doi:10.5194/acp-15-2031-2015, 2015.

Table 1. Mean concentrations of identified organic compound classes (ng m^{-3}) and carbonaceous components (μg m^{-3}) in the atmospheric aerosol samples ($PM_{2.5}$) from Nanjing, China.

Compounds	Daytime				Nighttime			
	Mean	Min[a]	Max[b]	SD[c]	Mean	Min[a]	Max[b]	SD[c]
n-Alkanes	177	96.1	467	76.6	218	74.4	500	89.3
Plant Wax Alkanes	15.5	1.12	56.2	11.2	17.6	0	62.1	14.2
Fatty acids	66.8	14.3	254	47.9	91.3	8.57	252	59.2
Fatty alcohols	36.9	7.30	165	29.9	43.8	4.61	129	26.7
Anhydro-sugars	42.3	5.8	191	40.9	71.2	5.71	367	80.1
Sugars	3.44	0.78	8.89	1.75	3.43	0.59	8.49	1.81
Phthalate esters	13.9	2.66	40.0	10.1	16.3	3.80	51.8	11.1
Glycerol and polyacids	7.78	1.59	29.7	6.17	9.30	2.54	23.1	5.79
Aromatic acids	6.70	1.53	23.1	4.69	8.37	1.99	18.4	4.83
Lignin and resin products	2.68	0.84	6.96	1.29	3.39	0.75	14.3	2.70
PAHs	54.5	29.5	106	17.8	74.8	21.7	223	43.8
Hopanes	3.79	0.07	20.8	4.15	4.64	0.13	26.1	5.31
Steranes	2.29	1.13	9.15	1.56	2.65	1.08	11.1	1.92
Total organics	**434**	**163**	**1378**	**254**	**565**	**126**	**1686**	**347**
OC	18.6	8.76	40.0	8.44	19.1	2.98	40.1	8.53
EC	8.25	2.41	30.3	5.46	8.86	8.86	8.86	8.86
WSOC	11.7	5.52	26.6	4.68	18.1	1.51	34.4	8.92
OC/EC	2.47	1.30	3.69	0.54	2.36	1.51	3.76	0.56
WSOC/OC	0.58	0.42	0.78	0.10	0.55	0.40	0.70	0.08

[a]Minimum, [b]Maximum, [c]Standard deviation

Table 2. Comparisons of the average concentrations (ng m^{-3}) of organic tracers with those measured during 2004-2005 (Wang and Kawamura, 2005; Wang et al., 2007a[b]) in Nanjing aerosols during winter.

Compounds	This study		2004-2005	
	Daytime	Nighttime	Daytime	Nighttime
n-Alkanes	177	218	172	278
Plant Wax Alkanes	15.5	17.6	18.8	20.6
Fatty acids	66.8	91.3	245	338
Fatty alcohols	36.9	43.8	74.5	120
Levoglucosan	42.3	71.2	238	297
Sugars	3.44	3.43	59	53
Phthalate esters[b]	13.9	16.3	158	181
Glycerol and polyacids	7.78	9.30	41.4	41.8
Aromatic acids	6.70	8.37		Not detected
Lignin and resin products	2.68	3.39	16.0	35.1
PAHs[b]	54.5	74.8	69	104
Hopanes[b]	3.79	4.64	7.3	9.9
Steranes	2.29	2.65		Not detected
Total organics	**434**	**565**	**1108**	**1502**

Table 3. Diagnostic concentration ratios of biomarkers for source identification from fossil fuel combustions including gasoline- and diesel cars.

	Present study		Gasoline		Diesel	Coal
	Daytime	Nighttime	Noncatalyst	Catalyst		
IP/BghiP	1.26	1.19	0.22[a]		0.50[a]	1.3[a]
BghiP/Bep	1.21	1.13	2.0[b]			0.8[b]
Flut/(Flut + IP)	0.57	0.56	0.46-0.56[c]	0.44[c]		
IP/(IP + BghiP)	0.56	0.54	0.18[c]		0.37[c]	0.56[c]
$C_{29}\alpha\beta/C_{30}\alpha\beta$	0.65	0.51	0.59[d]	0.66[d]	0.42[d]	0.58-2.0[e]
$C_{31}\alpha\beta S/(C_{31}\alpha\beta S + C_{31}\alpha\beta R)$	0.39	0.57	0.60[d]	0.62[d]	0.50[d]	0.05-0.37[e]

[a]Grimmer et al., 1983, [b]Ohura et al., 2004, [c]Bi et al., 2005, [d]Rogge et al., 1993a, [e]Oros and Simoneit, 2000

1159

1160

1161

1162

1163 **Figure 1.** A map of sampling site located in Nanjing, China.

1164

1165

1166

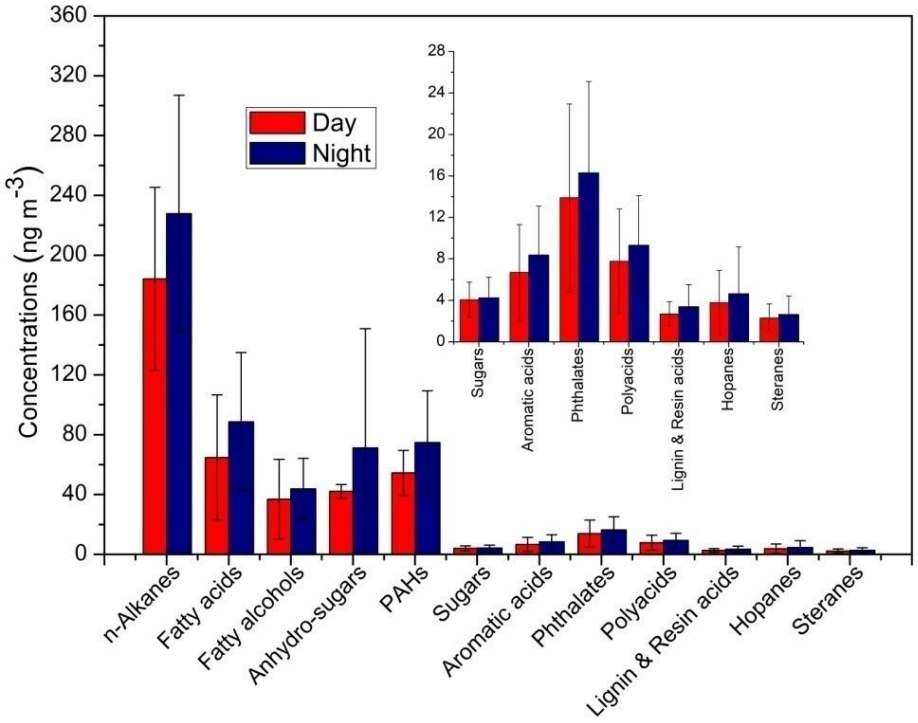

Figure 2. Concentrations of organic compound classes detected in the Nanjing aerosols.

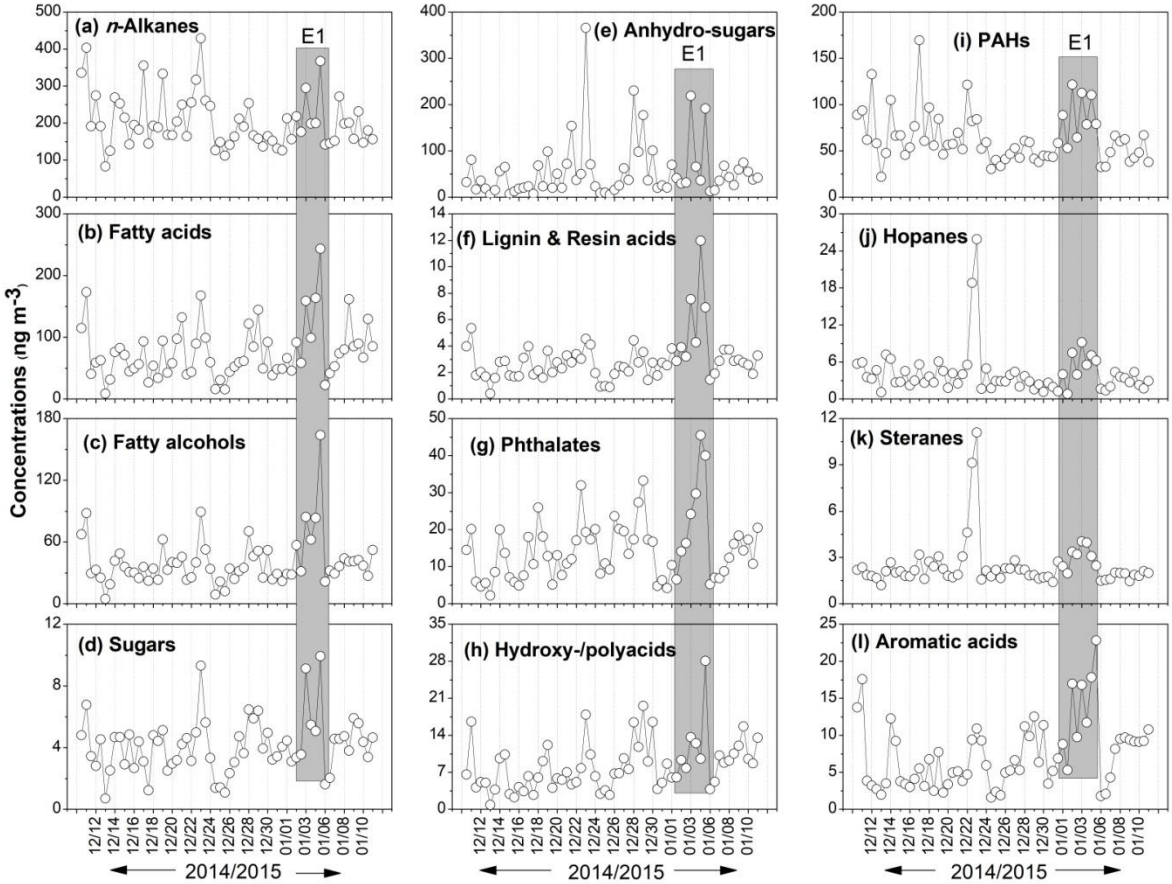

Figure 3. Temporal variations in the concentrations of organic compound classes detected in the Nanjing urban aerosols.

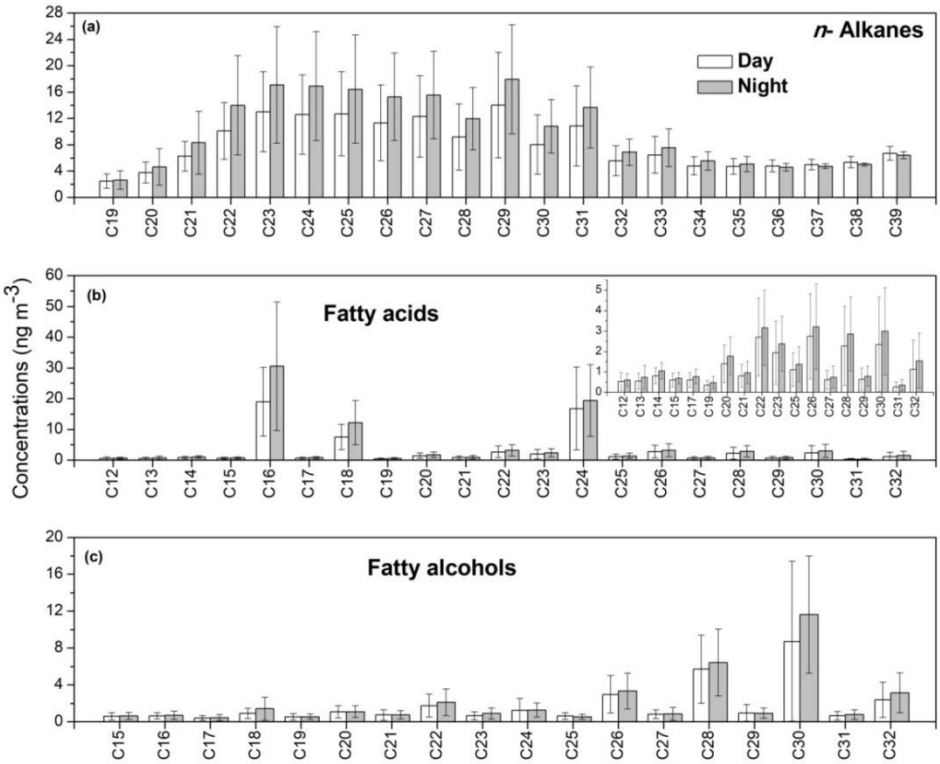

Figure 4. Molecular distributions of *n*-alkanes, fatty acids and fatty alcohols in $PM_{2.5}$ aerosols collected from Nanjing, China. Inner panel of b represent correspondence carbon of fatty alcohols which concentrations are low.

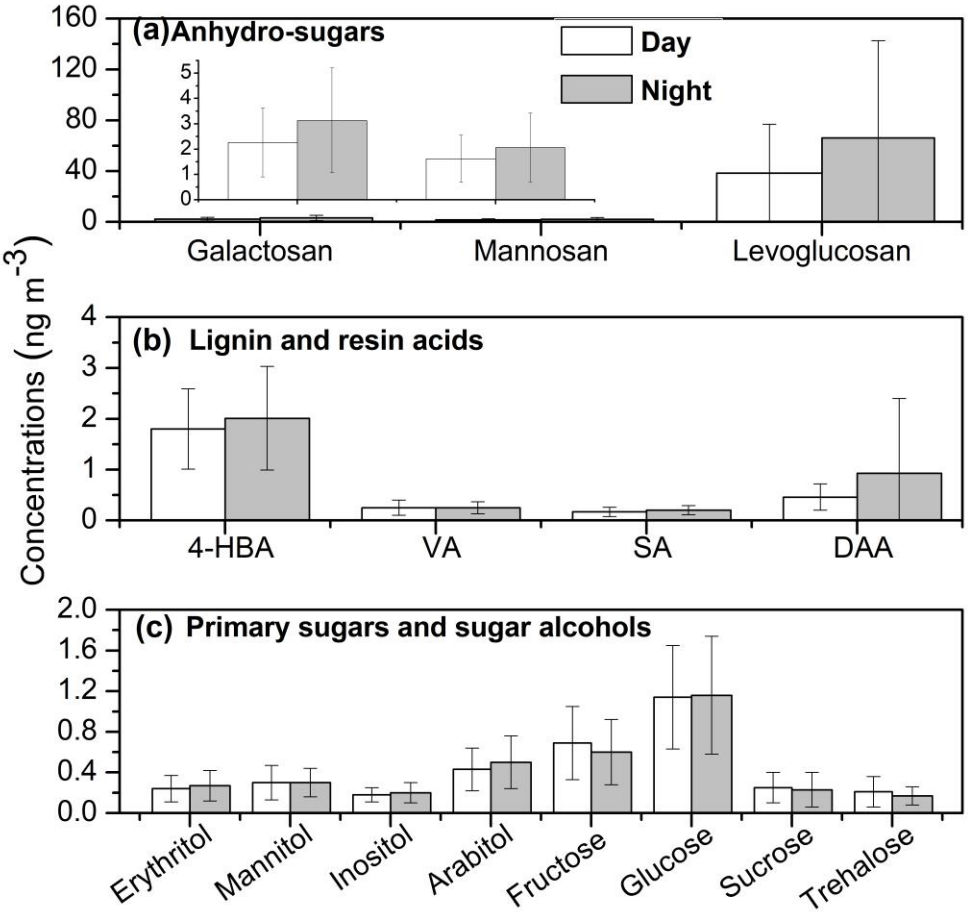

Figure 5. Molecular distributions of anhydro-sugars, lignin and resin acids and sugars/sugar alcohols in Nanjing aerosols. [4-HBA: 4-hydroxybenzoic acid , VA: vanillic acid, SA: syringic acid and DAA: dehydroabietic acid].

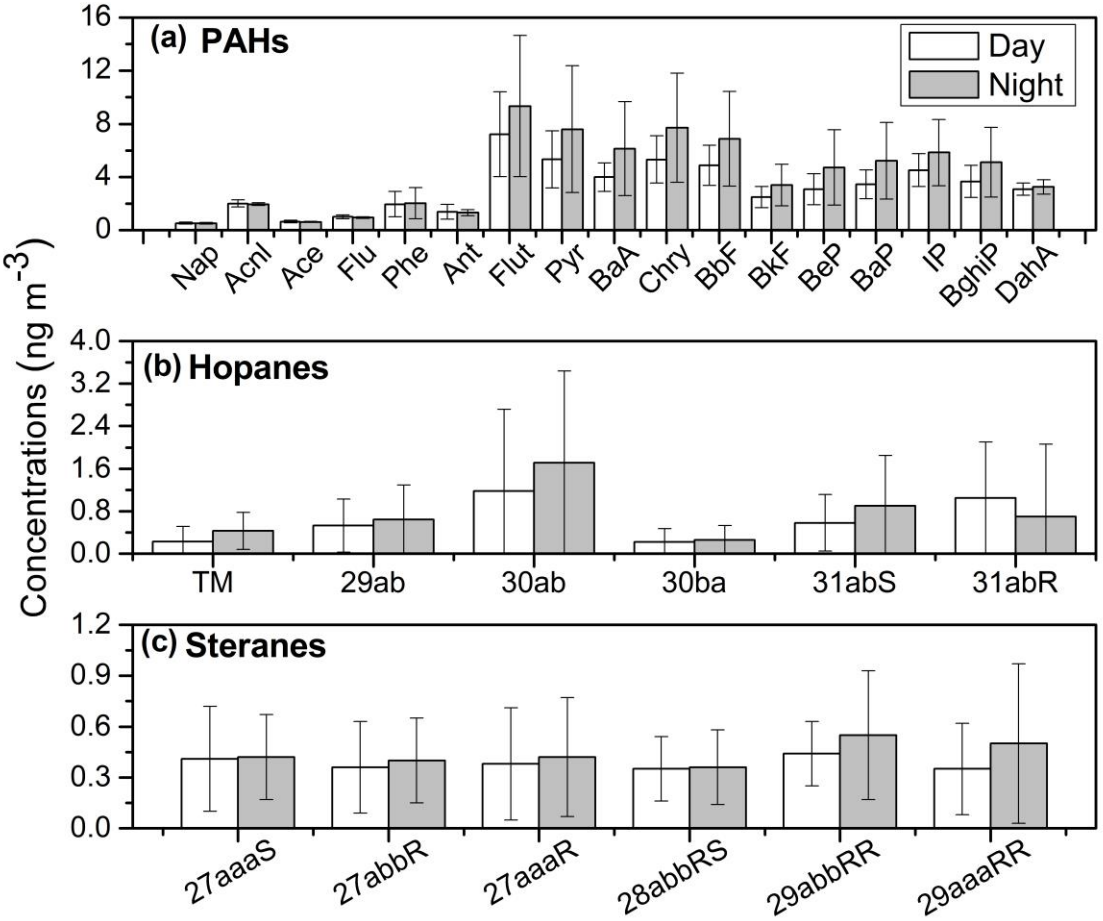

Figure 6. Molecular distributions of PAHs, hopanes and steranes in winter aerosols from Nanjing, China. [Abbreviation of PAHs: napthalene, Nap; acenaphthylene, Acnl; acenapthene, Ace; fluorene, Flu; phenanthrene, Phe; anthracene, Ant; fluoranthene, Flut; pyrene, Pyr; benzo[a]anthracene, BaA; chrysene, Chry; benzo(b)fluoranthene, BbF; benzo(k)fluoranthene, BkF ; benzo(e)pyrene, BeP; benzo(a)pyrene, BaP; indeno(1,2,3-cd)pyrene, IP; benzo(ghi)perylene, BghiP; Dibenzo[a,h] anthracene, DahA].

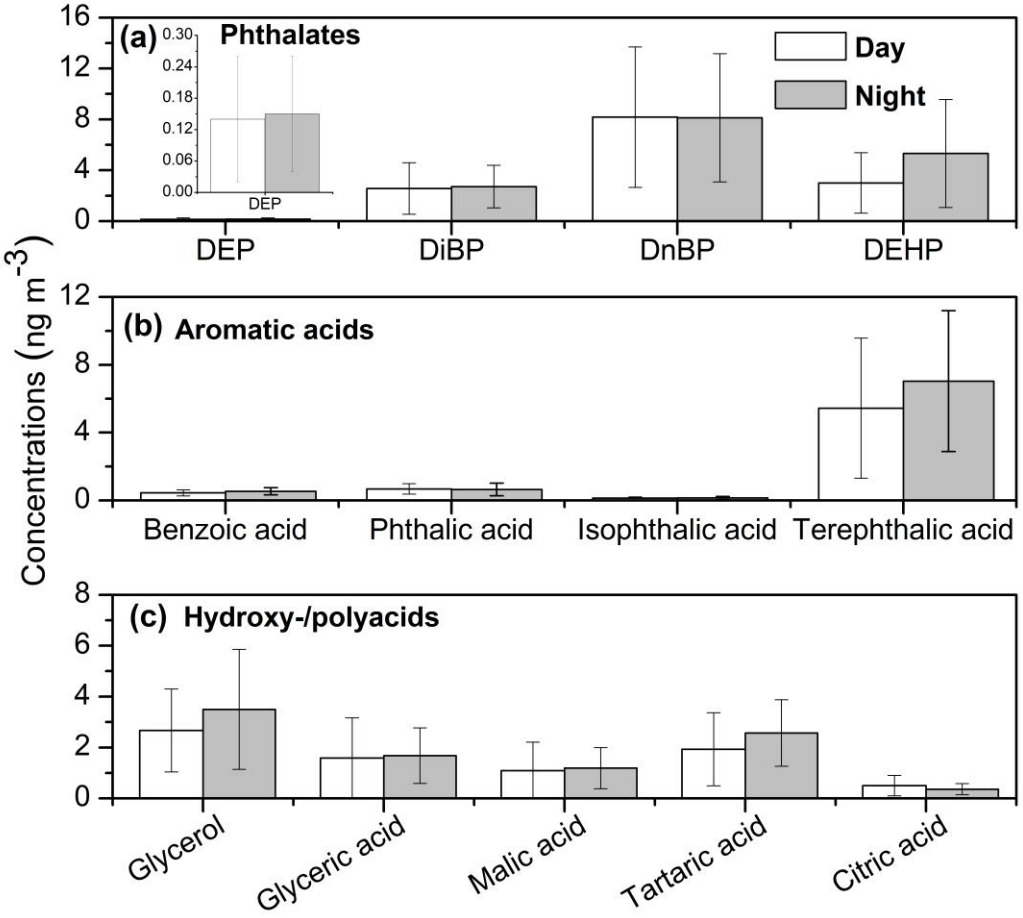

1199

1200 **Figure 7.** Molecular distributions of phthalates, aromatic acids and hydroxy-/polyacids in
1201 Nanjing aerosols.

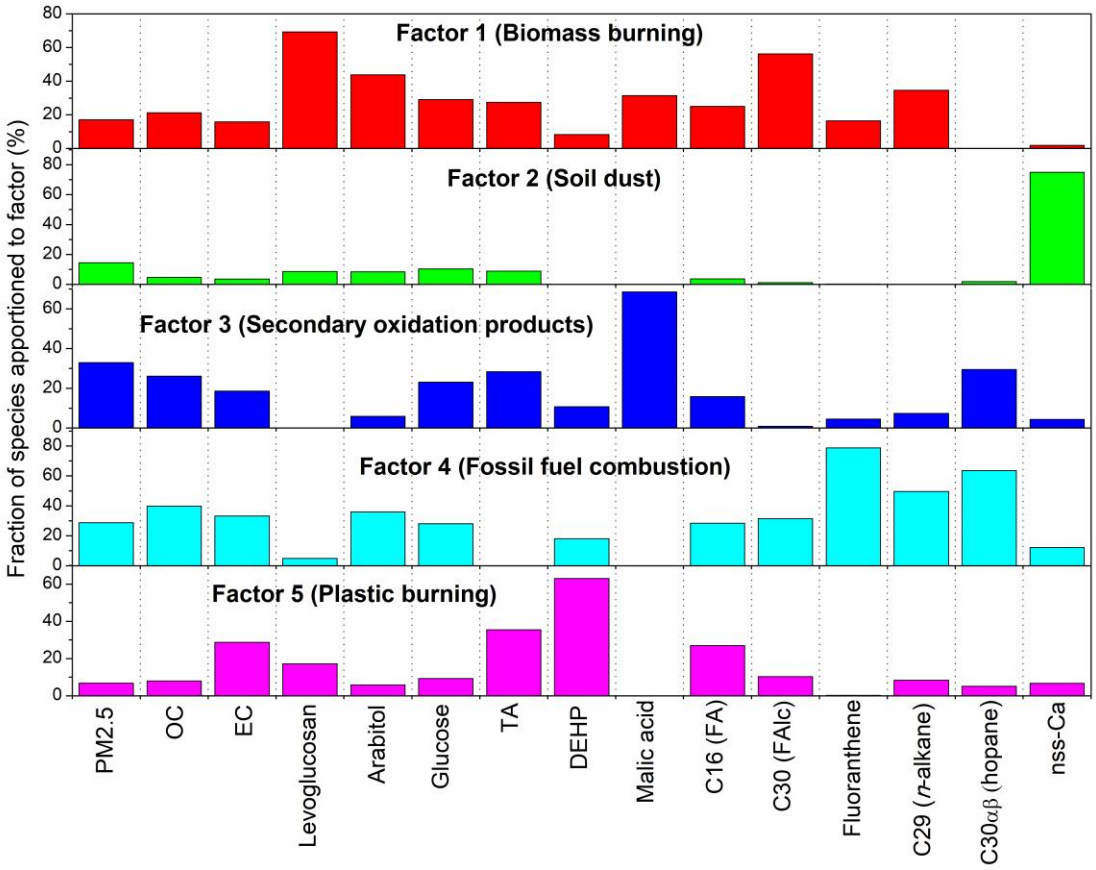

Figure 8. Composition profiles (% of total of each species) for the five factors resolved by PMF based on data from Nanjing winter aerosols from 11 December 2014 to 11 January 2015. [TA: terephthalic acid, DEHP: di-(2-ethylhexyl) phthalate, FA: fatty acid, FAlc: fatty alcohol].

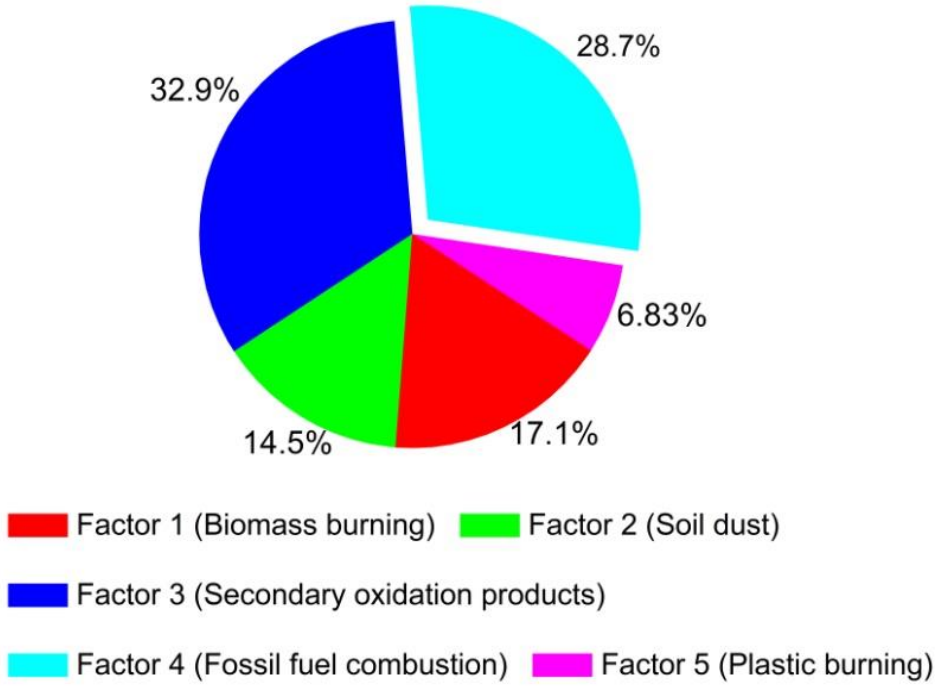

Figure 9. Pie diagrams showing the estimated source contributions of five factors resolved by PMF to the $PM_{2.5}$ in Nanjing aerosols.